Physics – Uspekhi **61** (4) 323 – 352 (2018)

REVIEWS OF TOPICAL PROBLEMS

PACS numbers: 61.05.fg, **61.46. – w**, 75.50.Mm

100 years of the *Uspekhi Fizicheskikh Nauk* journal

Solar cosmic rays: 75 years of research

L I Miroshnichenko

DOI: https://doi.org/10.3367/UFNe.2017.03.038091

Contents

Abstract. The 28th of February 2017 marked the 75th anniversary of the first confident detection of solar cosmic rays (SCRs), a term referring to accelerated solar particles with energies from about 10^6 to $\sim 10^{10} - 10^{11}$ eV. The present paper reviews the key observational and theoretical results on SCRs that have been accumulated over this period. The history of the discovery of SCRs is briefly described, together with SCR recording techniques and instruments, and some physical, methodical, and practical aspects of SCR generation are discussed in more detail. Special attention is given to mechanisms of charged particle acceleration at and near the Sun. Current ideas on the interaction of solar cosmic rays with the solar atmosphere, peculiarities of their transport in interplanetary magnetic fields, movements in Earth's magnetosphere, and their impact on Earth's atmosphere are reviewed. It is shown that this field of space physics has produced many results of fundamental interest for astrophysics, solar–terrestrial physics, geophysics, and practical cosmonautics (astronautics).

L I Miroshnichenko Pushkov Institute of Terrestrial Magnetism, Ionosphere and Radio Wave Propagation (IZMIRAN), Russian Academy of Sciences, Kaluzhskoe shosse 4, 108840 Troitsk, Moscow, Russian Federation; Lomonosov Moscow State University, Skobeltsyn Institute of Nuclear Physics, Leninskie gory 1, 119991 Moscow, Russian Federation
E-mail: leonty@izmiran.ru

Received 29 December 2016, revised 28 February 2017
Uspekhi Fizicheskikh Nauk **188** (4) 345 – 376 (2018)
DOI: https://doi.org/10.3367/UFNr.2017.03.038091
Translated by Yu V Morozov; edited by A Radzig

Keywords: Sun, solar flares, particle acceleration, solar cosmic rays

Main abbreviations:
PC — prompt SCR component
BUST — Baksan Underground Scintillation Telescope
GCR — galactic cosmic rays
GSMF — global solar magnetic field
IC — ionization chamber
CME — coronal mass ejection
CR — cosmic rays
IGY — International Geophysical Year (1957–1958)

DC — delayed SCR component
IMF — interplanetary magnetic field
MT — muon telescope
NM — neutron monitor
SA — solar activity
CE — the Carrington event
SCR — solar cosmic rays
SNT — solar neutron telescope
SPE — solar proton event
CS — current sheet
ACE — Advanced Composition Explorer (spacecraft)
ACS — Anti-Coincidence Shield for Integral spacecraft
BDE — Bastille Day event (proton event of 14 July 2000)
CI — coronal index
FD SOC — fractal-diffusive self-organized criticality (model)
GLE — ground level enhancement (proton event)
GOES — geostationary operational environmental satellite (geostationary satellite)
NMDB — Neutron Monitor Database
NOAA — National Oceanic and Atmospheric Administration
SEC — Space Environment Center
PFSS — Potential Field on Source Surface (model)
pfu — proton flux unit (1.0 pfu = 1 proton/(cm^2 s sr)
SEP — solar energetic particle
SFI — solar flare index
UT — Universal Time

1. Introduction

Charged solar particles accelerated up to energies from about 10^6 to $\sim 10^{10}-10^{11}$ eV and known by the longstanding traditional name 'solar cosmic rays' (SCRs) have been studied by various methods already for 75 years. They were registered for the first time in February 1942 [1], i.e., 30 years after the discovery of galactic cosmic rays (GCRs). However, as soon as within the next 15 years the SCR studies gave rise to a separate successful research area in space physics. Running somewhat ahead, it should be noted that SCR investigations resulted in the discovery of at least two fundamental processes in outer space. One concerns the acceleration of particles up to relativistic energies in the solar atmosphere, i.e., SCR generation, considered in the present review article. The other process covers the generation of shock waves in the interplanetary plasma manifested as reduced GCR intensity (the so-called Forbush effect). Both processes are due to energetic solar events [2].

Primary cosmic rays (CRs) entering Earth's atmosphere destroy nitrogen and oxygen nuclei (the most abundant elements in the atmosphere) and induce a nuclear cascade process giving rise to numerous secondary particles (secondary CRs). SCRs approaching Earth cause a sharp increase in the secondary CR flux observable on Earth's surface. Such an increase is referred to as a ground level enhancement (GLE).

The very first SCR events were usually registered as statistically significant enhancements of secondary CR fluxes against the background of GCRs. At first, such episodic phenomena were considered in the framework of a more general problem of CR variations at large (e.g., Refs [3–5]). Later on, comprehensive reviews [6, 7] and the first monographs [8, 9] were published. Today, the literature on SCR amounts to hundreds of original and review articles, Refs [10–16] being the mostly frequently cited among them in the last few years. In addition, recently released monographs [17–20] are concerned with various methodical, experimental, and general physical aspects of SCR research, peculiarities of SCR interaction with the solar atmosphere, geophysical SCR effects, their potential influence on solar–terrestrial relationships, and current applications of SCRs. An important contribution to SCR exploration has been made by researchers of the Institute of Terrestrial Magnetism, the Ionosphere, and Radio Wave Propagation (IZMIRAN), which has recently celebrated its 75th anniversary [21].

The present review, preceded by a brief historical introduction, was designed to discuss updated theoretical (model) and observational data that the author considers to be of special importance for further research and potential applications. He is fully aware that it is impossible to comprehensively examine the current situation in this rapidly developing field of space physics within the scope of a single report. This shortcoming is believed to be partly made up for by an assortment of illustrations and references to original investigations.

2. The Sun as a source of cosmic rays

2.1 Short history of the discovery and methods of registration

The history of science gives evidence that the birth of a new scientific field cannot be fixed to any concrete date except in a few cases. But this is exactly what happened in the case of SCRs; namely, a ground detector recorded for the first time accelerated (relativistic) particles coming to Earth from the Sun on 28 February 1942. In a week (7 March 1942), an analogous event took place again [1]. It was a major astrophysical discovery of the 20th century. It turned out that charged particles present in the stellar atmosphere can be accelerated up to very high (relativistic) energies. True, the researchers did not immediately comprehend the significance of this fundamental fact and its close relation to solar flares. The authors of Ref. [1] attributed CR variations observed on 28 February and 7 March 1942 to perturbations in Earth's magnetosphere. Only a third event that occurred on 25 July 1946 enabled the observer in paper [22] to come cautiously "...to the unexpected conclusion that all the three unusual enhancements in CRs can be ascribed to charged particle fluxes emitted from the Sun". Then, a fourth enhancement documented on 19 November 1949 [23–25] made the association of accelerated relativistic particles with solar flares an unquestionable fact that provided the basis for a novel paramount scientific concept.

Since the turn of the 1990s, the term ground level enhancement or ground level event (GLE) has been universally accepted to define this phenomenon [2, 26]. For convenience, all such events have been given serial numbers, starting from GLE1 recorded on 26 February 1942. A total of 71 GLEs have been documented over 75 years (February 1942–February 2017). They are extensively investigated at many world centers. A special issue of *Space Science Reviews* (vol. 171) published in 2012 contained seven articles by foreign authors on different aspects of GLE research; such great and universal interest in the phenomenon in question reflects its fundamental character.

In the same year of 1942 (26–28 February), British radio engineers tracking German submarines observed for the first time intense radio noises (radio outbursts) in the meter wave range (4–6 m) coming from the direction of the Sun [27]. As it

later turned out, this radiation produced by accelerated electrons originated from the active region that crossed the central solar meridian (CSM). To all appearances, the powerful 3+ solar flare (07°N, 04°E) occurred precisely in this region on 28 February 1942 [10, 11]. Thus, in addition to the discovery of SCRs, another historic event in solar research occurred in February 1942 — that is, the birth of solar radio astronomy, even though it was first reported only in 1946 [28].

There are many other types of solar activity besides flares and radio outbursts, viz. solar flares and spots, prominences, coronal mass ejections, coronal holes, etc. In general terms, solar activity (SA) is a continuum of events and processes related to the formation and decay of strong magnetic fields in the solar atmosphere, conversion of their energy into matter motion energy, energies of accelerated particles, and different forms of electromagnetic radiation.

In the 1940s, data on SA manifestations in the atmosphere of Earth, such as geomagnetic storms, auroras, ionospheric perturbations, and the like (e.g., as sources of natural interference to detection and tracking radio-technical systems) were shrouded in secrecy by the antagonists in the World War II (1939–1945) [29]. Moreover, CR studies were at that time the realm of nuclear physics, and their results were either partly (USA) or totally (Germany, USSR) shrouded in a veil of secrecy as being related to the development of nuclear weapons [30, 31]. Certain research teams observed between 1941 and 1943 other manifestations of enhanced CR intensity reminiscent of solar flare effects [27]. But only after the 1946 and 1949 ground level events had been documented was the hypothesis of their solar origin recognized as an indisputable scientific fact.

It was the first substantial result achieved in this field; namely, a basic astrophysical phenomenon, such as acceleration of charged particles (protons), was shown to occur in outer space (stellar atmospheres). To recall, the discovery had been made before 1953 when cosmic magnetic bremsstrahlung (synchrotron radio emission) was observed in the Crab Nebula, suggesting that similar electron acceleration processes take place in the Galaxy, e.g., in supernova explosions. Importantly, SCR studies originated with the analysis of ground-based observations some 30 years after the breakthrough discovery of galactic cosmic rays by V Hess in August 1912 (see, for instance, original report [32]) and the historical sketches [33, 34]). Notice that the nature of GCRs remained unclear up to the 1940s.

2.2 Modern databases

Ground-based observations of secondary components (mostly muons and neutrons) thus far remain the most reliable source of information about primary relativistic SCRs. The historically first detectors for registering SCRs were ionization chambers (ICs) and muon telescopes (MTs). Neutron monitors (NMs) found application in the mid-1950s. When used to record GCRs at sea level, these standard detectors had the effective energies of $\sim 25-35$, 15–20, and 4–6 GeV, respectively [17]. Neutron detectors of SCRs were employed for the first time to register the event on 19 November 1949 [23]. A worldwide network of NM-based stations for continuous registration of CRs was set up over 50 years ago [4, 5]. Their important characteristic is limiting magnetic rigidity (limiting energy) of the particles arriving at the atmospheric boundary layer over a given point on Earth's surface (the so-called geomagnetic cutoff rigidity R_c of particles traveling in Earth's magnetosphere). The particle magnetic rigidity $R = cp/Ze$ stands for the momentum unit p per charge unit Z (c — speed of light, and e — electron charge); it is usually measured in volts, megavolts, and gigavolts). The relationship between magnetic rigidity and particle energy is described in Section 3.1.

Efforts to continually improve systems for data collection with NMs and their analysis ended in the creation of an SNM-64 neutron supermonitor [35]. The statistical measurement error of this instrument per hour of registration during the period of solar minimum (i.e., maximum GCR intensity) at the Apatity station (67.57°N, 33.4°E, 181 m above sea level, $R_c = 0.65$ GV) was 0.246% or roughly thrice that of the IGY type neutron monitor (0.81%). For the Moscow station (Troitsk, 55.47°N, 37.32°E, 200 m above sea level, $R_c = 2.44$ GV), the registration accuracy was close to 0.18%, compared with $\sim 0.36\%$ for Mexico City (2274 m above sea level, 99.2°W, 19.33°N, $R_c = 8.2$ GV). In other words, the accuracy depends on the altitude above sea level, the latitude of the station (to be precise, its R_c), and the number of SNM-64 counters in a given detector (which may vary). The high statistical accuracy allows the 'fine structure' of SCR time profiles during GLE to be measured with a resolution of 1 min and even 10 s, then constructing improved models of emission, acceleration, and propagation of SCR fluxes.

The present-day worldwide network of NM-based stations for continuous registration of CRs (Fig. 1) consists of approximately 50 stations equipped mainly with SNM-64 supermonitors, the data from which form the international Neutron Monitor Database (NMDB, http://www.nmdb.eu); see also the international GLE Database (http://gle.oulu.fi). There are ground-based MTs differing in design that allow recording SCRs incident at large angles with respect to the vertical. In addition, there are several underground MTs making possible registration of extreme events like the GLE that occurred on 29 September 1989 (GLE42) (see Refs [36–38]). Sometimes, GLEs produce secondary muon outbursts registered by nonstandard devices designed to address astrophysical problems and/or examine nuclear physical effects of GCRs [39]. These observations are supplemented by the data coming from a network of solar neutron telescopes (SNTs) [40] that register arrival of secondary neutrons produced in the solar atmosphere by primary accelerated ions.

Information gathered by the worldwide network of NM-based stations permits the maximum energy E_m of SCR (or maximum magnetic rigidity R_m of an accelerated particle) to be evaluated practically at the upper limit of the range (i.e., near $R_c = 17$ GV at the geomagnetic equator). By way of example, standard detectors gave $R_m = 20.0(+10, -4)$ GV for the event recorded on 23 February 1956 (GLE05), the largest throughout the entire history of observations. The use of nonstandard detectors opens up an attractive possibility [41] for penetrating into the region of energies much higher than 20 GeV. Specifically, the use of inclined muon telescopes in India allowed the presence of relativistic solar protons with energies falling within the range 35–67.6 GeV in the same GLE05 event to be revealed. Observations with underground MTs oriented toward the Sun suggest the possibility of accelerating solar protons to energies $E_p \approx 200$ GeV [42], and even to $E_p \geqslant 500$ GeV [39]. However, the latter possibility, while so very tempting, remains to be doubtful.

GLE-like events (kinetic energy $E_p \geqslant 433$ MeV/nucleon or magnetic rigidity $R \geqslant 1$ GV) characterize only one, relativistic, part of the total SCR spectrum. Neutron monitors are practically insensitive to primary protons having energy $E < 100$ MeV

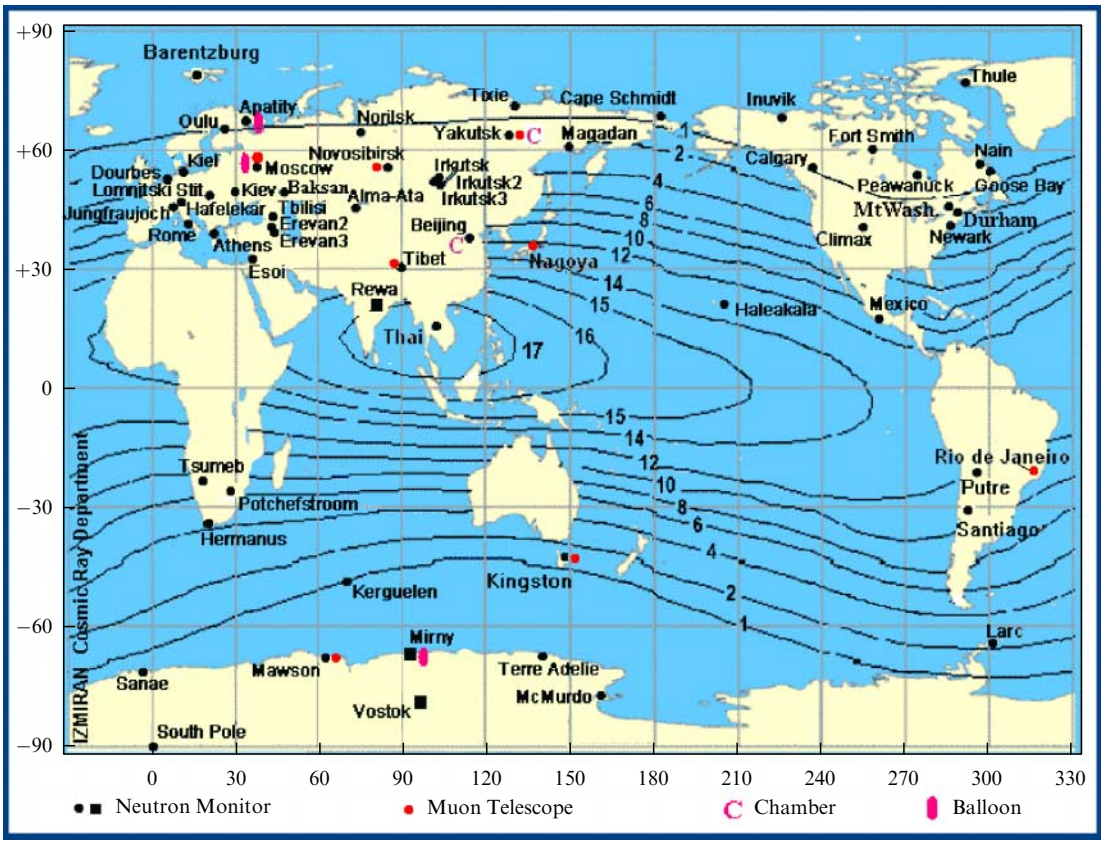

Figure 1. (Color online.) The worldwide network of stations for continuous registration of cosmic rays of galactic and solar origin (GCRs and SCRs). The numbers alongside the curves correspond to isolines for geomagnetic cutoff rigidity of primary cosmic particles (in GV units) (figure taken from the IZMIRAN website http://crO.izmiran.ru/common/NetMapOO.gif, with modifications.

($R < 0.44$ GV), because secondary neutrons are absorbed in the atmosphere (the so-called 'atmospheric cutoff', R_a, threshold), the maximum sensitivity of NMs lying within the 1–5 GV range. This means that all high-latitude (polar) stations begin to register secondary neutrons at the same rigidity of primary protons of ≈ 1 GV, regardless of the nominal value of calculated geomagnetic cutoff rigidity R_c for a given NM. Fortunately, the rigidity value of ≈ 1.0 GV (~ 433 MeV) proved to be intermediate between the values for nonrelativistic and relativistic proper SCRs; it therefore can serve as a convenient reference value of the rigidity threshold for polar NM stations [43].

Figure 2a presents time profiles of ground level enhancements of solar cosmic rays for the first three GLEs [22] obtained with the aid of an ionization chamber at the Cheltenham station (USA). Figures 2b, c show the last event of the 23rd cycle — GLE70 (13 December 2006). Interestingly, it was recorded not only by the worldwide NM network (see Refs [44, 45]) but also by certain nonstandard ground-based detectors, e.g., the URAGAN wide-aperture large-area multilayer muon hodoscope [46] and the IceTop detector of extensive air showers (EAS), a component of the IceCube neutrino telescope submerged in the Antarctic ice [47].

Direct spacecraft measurements near Earth's orbit (1 AU from the Sun) performed since the 1960s made it possible to register solar energetic particles (SEPs) in the $E \geqslant 0.5$ MeV/nucleon region. Such solar energetic particle fluxes are now called solar proton events (SPEs). The SPE occurrence rate η was found to rapidly increase with decreasing threshold registration energy. For example, the rate of SPEs (GLEs) for energy $E \geqslant 433$ MeV/nucleon ($R \geqslant 1$ GV) was shown to be $\eta \approx 1.0$ year^{-1}; it increased to 2.0 year^{-1} for $E \geqslant 100$ MeV/nucleon, and to $\eta \geqslant 250$ year^{-1} for $E \leqslant 10$ MeV/nucleon (for protons). The lowered registration threshold, increased sensitivity of detectors, and prolonged duration of spacecraft-based measurements taken together give evidence that the Sun is actually a continuous source of SEPs with energies $E \geqslant 1$ MeV/nucleon [13, 20]. It can be argued that the spectrum of GLE particles is a continuation of the general SCR spectrum (beginning from approximately $E \geqslant$ 1–10 MeV/nucleon) into the relativistic region.

2.3 Two paradigms of solar–terrestrial relationships

In the early 1990s, solar–terrestrial physics, which encompasses heliophysics and geophysics, went through a number of important changes. To begin with, the phenomenological concept of coronal mass ejection (CME) had finally been formulated in the USA by that time. Closely related to the CME concept is the well-known paradigm of SCR acceleration at shock wave fronts. Despite being of questionable value, it is advocated by many researchers, especially in the USA, who discard the earlier hypothesis of particle acceleration in solar flares during magnetic reconnection (see Sections 4.1–4.4 for a detailed discussion of these issues).

The discovery of CME prompted certain researchers to revise the basic paradigm of solar–terrestrial relationships. The author of Ref. [48] proposed that CME (rather than solar flares) be considered the main factor (cause) of the Sun's

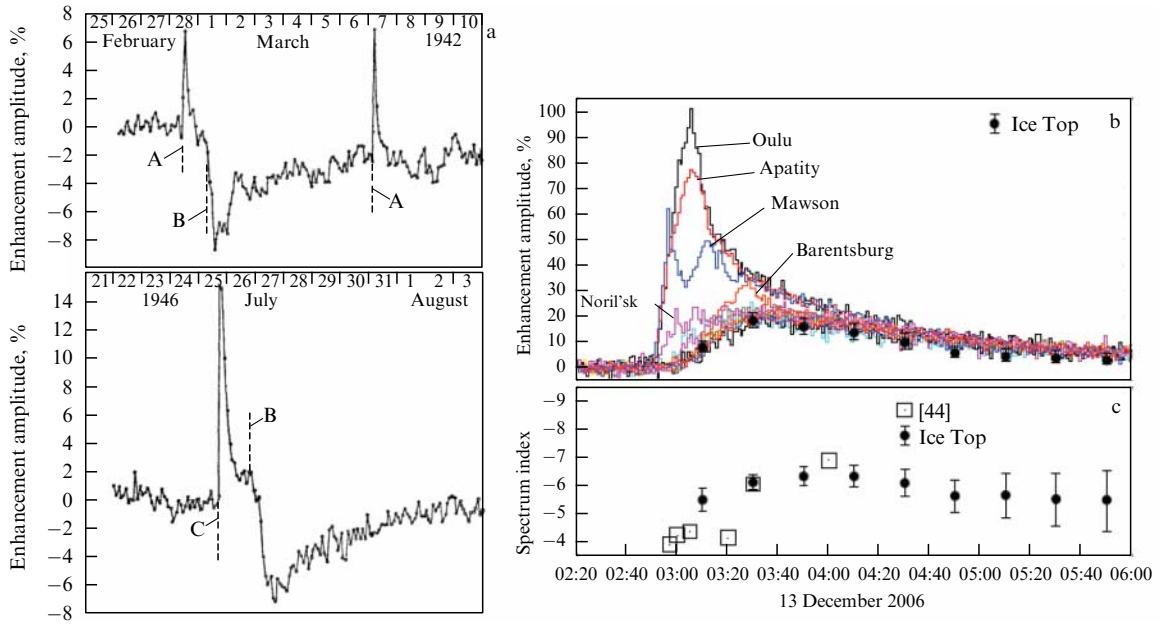

Figure 2. (Color online.) (a) Results of observations at the Cheltenham station (USA) for the first three GLEs [22]; A — onset times of radio fadings, B — onset times of magnetic storms, C — onset time of the solar flare (25 July 1946). (b, c) Results of observations of GLE70 by the worldwide network of stations (b) and comparison of the SCR spectrum index in Earth's orbit (c) evaluated from the data obtained with NMs [44] and the AES IceTop detector, part of the IceCube neutrino telescope (Antarctica) [47].

influence on Earth and 'space weather' (magnetic storms, ionospheric perturbations, radiation environment of Earth, etc.). "The Solar Flare Myth" became the subject of ardent debates in the literature and at the scientific conferences (see, e.g., Refs [13, 38]). The new paradigm of cause-and-effect relationships in solar–terrestrial physics displaced the solar flare from its central position as the main cause of perturbations in near-Earth space. It was superseded by coronal mass ejection. Flares give rise to weak and short (impulsive) enhancements of particle fluxes, whereas in powerful and long-term (gradual) events, SCRs are accelerated at the shock wave front associated with coronal mass ejection. The author of Ref. [48] maintained that gradual events are totally unrelated to solar flares. Although CMEs were discovered as early as 1971, they were not even mentioned in the joint article [49] published on the occasion of the 50th anniversary of IZMIRAN (1989): the term 'coronal transients' was in use at that time.

Today, increasingly more specialists tend to believe that solar flares and CMEs are two sides of the same phenomenon — explosive perturbation in the solar atmosphere releasing a great amount of energy (Fig. 3). Evidently, this is a fundamental astrophysical problem in which topological links between the magnetic fields of flares and CMEs are as important as the physical links (see also Section 9.2)

An indispensable constituent component of an explosion is the generation of high-energy particles, i.e., SCRs with a proton energy of $\geqslant 1$ MeV. They are often referred to as solar energetic particle (SEPs). In what follows, this acronym will be used largely in the description of the SCR nonrelativistic fraction, whereas the term GLE particles is reserved to define the relativistic part. To avoid confusion, it is worthwhile to underscore once again that the terms SEP and SCR are common for the whole variety of accelerated solar particles, with GLE particles representing the extension of the SEP spectrum into the region of relativistic values.

Figure 3. (Color online.) Eruptive energy release in the solar atmosphere (as represented by a NASA/MSFC artist). A bright flare in the region of reconnection of oppositely directed magnetic fields (red and blue lines); part of the energy is transferred to coronal mass ejection (Image credit: NASA/MSFC).

Figure 4 illustrates one of the proton events of current solar activity cycle 24 recorded on 17 May 2012 (GLE71). Despite the low intensity, it was readily measured by both ground-based detectors and several spacecraft (e.g., WIND, ACE, GOES 13). The beginning of the GLE was characterized by strong SCR anisotropy.

The analysis of multiwave observations of the images of an exploding prominence and CME enabled the authors of Ref. [50] to obtain evidence that protons with an energy of up to ~ 1.12 GeV in GLE71 could be accelerated by a shock wave resulting from the CME in the corona at heights of up to ~ 3.07 solar radii. It is noteworthy, despite the apparent ambiguity of this conclusion, that the near-Earth time-of-maximum (TOM) spectrum corresponding to the SCR

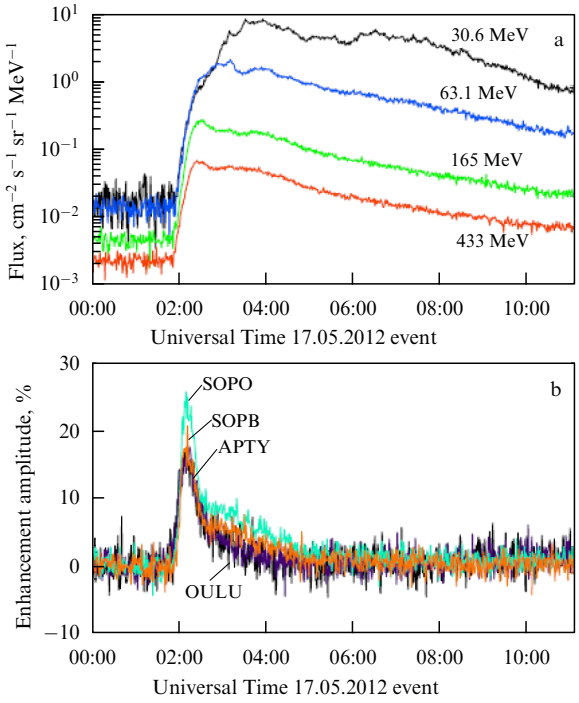

Figure 4. (Color online.) SCR intensity–time profiles during the 17.05.2012 event measured aboard the GOES 13 spacecraft. (a) (http://www.ospo.noaa.gov/Operations/GOES/13/index.html) and data from ground-based NMs (b) (Neutron Monitor Data Base (NMDB, http://www.nmdb.eu).

spectrum in the source has a typical shape characteristic of shock acceleration.

2.4 Heliolongitudinal effects in the nonrelativistic region

It follows from the foregoing that solar energetic particles can originate from different sources at or near the Sun, with absolute SEP fluxes, intensity–time profiles, and spectral and angular characteristics varying from one event to another. These variations partly depend on the relative positions of the particle source and the point of observation. When a CME-generated shock wave serves as the source, asymmetry of the time spectrum shape seen in the Earth orbit (Fig. 5) is quite apparent, depending on whether the source is located at a west or east heliolongitude with respect to the CME and the shock wave. Such a picture emerges from the data obtained during 20 years of observations of 235 proton events with an intensity above 10^{-2} (cm^2 sr s MeV)$^{-1}$ in the energy range from 1 to 23 MeV (for protons) [51].

Let us assume that an observer sees the CME from a western source (W53°). At this moment, the observation point is lined up with the front part of the shock wave that still remains near the Sun. By the time at which the shock wave reaches Earth's orbit (1.0 AU), the observer will find himself at a 53° angle to the nose of the wave in the direction to its left flank, in fact, on the tubes of force that in the course of time turn out to be connected with a weaker source of particles, so that their intensity will decrease steadily. This decrease is an inevitable consequence of process geometry, even if neither velocity nor degree of compression in all parts of the shock wave changes with time. The point of magnetic connection of an observer with the wavefront move under such conditions eastward.

Near the center (E01°), the observer can see the slow initial phase of the event, because in this period he is connected with the western flank of the wave. However, in the case of a marked longitudinal extension of the CME, it is possible to see from his point of observation a flat time profile corresponding to virtually constant acceleration. Immediately behind the front, the intensities fall by an order of magnitude or even more as the observer sinks to the CME proper, where many lines of force remain tied to the Sun at both ends.

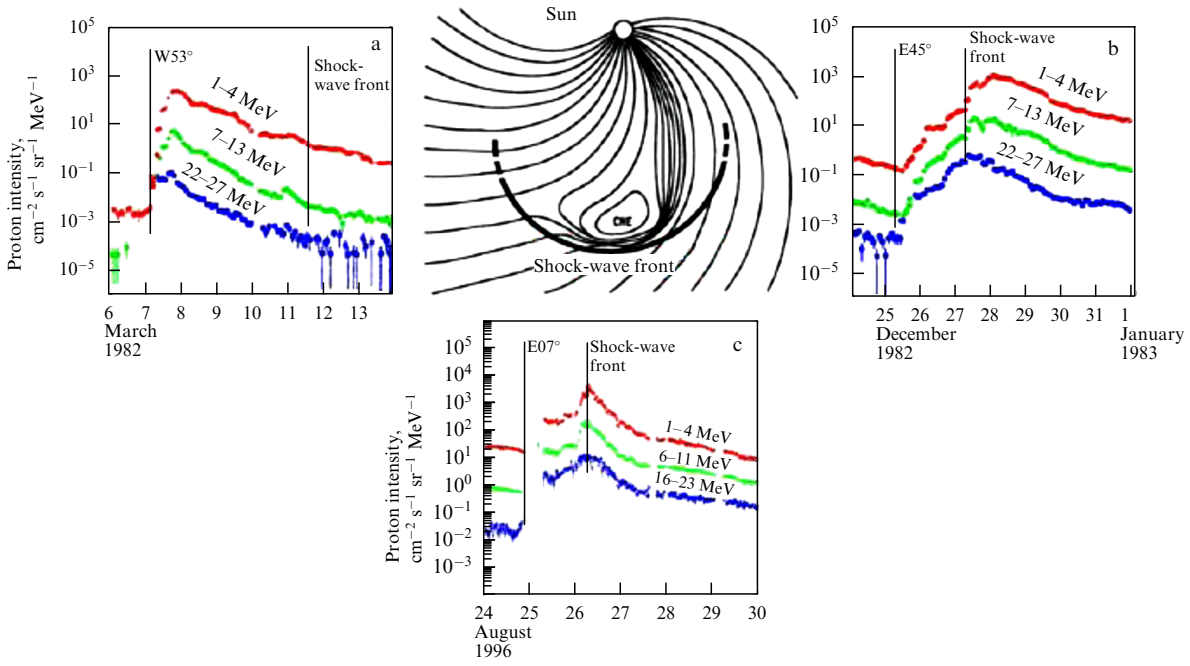

Figure 5. (Color online.) Dependence of SCR time profiles near Earth on the heliolongitude of solar sources. Typical SEP intensity–time profiles in Earth's orbit for three proton events observed at different heliolongitudes with respect to the CME and shock wave positions [51]. Profile asymmetry depending on source location: (a) west longitude W53°, (b) east longitude E45°, (c) a source at E07° longitude (near the center of the solar disk).

Finally, let us consider a situation in which the observer resides at the western flank of the wave (E45°). In this case, intensities may grow slowly as the wave approaches the base of the observer's force line inside the corona, far west of the particle source. The intensities grow as the connection point becomes displaced eastward toward the nose of the wave. However, peak intensities will be reached only after the observer crosses the front at 45° to the west of the nose of the wave and eventually places himself on the lines of force linking him to the nose of the shock-wave front from behind. Certainly, both the CME and the wave front are subject to irregular distortions of shape, but it seems very likely that particles are most efficiently accelerated near the central (nose) part of the wave where it is especially strong and the velocity in all likelihood is highest.

2.5 Heliolongitude of GLE sources

Complete GLE statistics (71 events) collected during 75 years of ground-based observations of SCRs provide a basis for addressing some questions pertaining to spatio–temporal variations of solar activity and properties of the global solar magnetic field (GSMF). Of special interest is GLE distribution over the heliolongitude of their sources (flares). It was established that the interplanetary magnetic field (IMF) is a guiding factor in the formation of SCR fluxes. Although relativistic particles traveling toward Earth as a rule do not undergo appreciable scattering (sometimes, their transport path may be compared to 1.0 AU), but the probability of reaching Earth strongly depends obviously on the Parker spiral angle of the IMF. This accounts for the strong dependence of registration rate η on the source heliolongitude: most sources are confined within a heliolongitude range of $\sim 30°\text{W}-90°\text{W}$ (Fig. 6). Amazingly, SCRs from even post-limb sources are known to have reached Earth in 12 cases. A similar distribution is documented for sources of the majority of nonrelativistic SPEs.

SPE sources presumably related to acceleration by shock waves in the interplanetary space are distributed more uniformly with a maximum at $\sim 30°\text{W}$ heliolongitude [17].

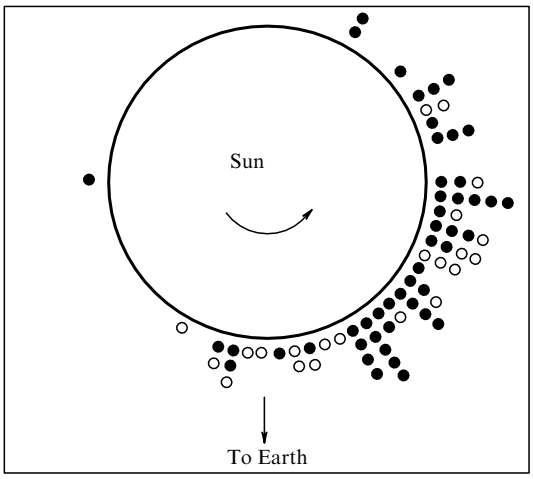

Figure 6. Heliolongitude distribution of GLE sources over the Sun's disk registered in 1956–1991 (dark dots) [52] and supplemented by the author [20] for events observed before 1956 and after 1991 (circles). A total of 70 events throughout the entire observation period (1942–2006) (viewed from Earth; arrow shows east–west rotation of the Sun).

2.6 Classification of events

A great variety of SPEs (including GLEs) observed in Earth's orbit, differing in energy spectra, intensities, elemental composition, charge states of accelerated particles, their spatial and temporal characteristics (variations), create serious difficulties encountered in the classification of events. Up to now, the best system for the purpose has been that of quantitative classification based on the intensity threshold proposed in the early 1970s [53] for protons with energies $E \geqslant 10$ MeV. This system provided a basis for SPE catalogs for the period from 1955 till 2008 [54–60). The catalogs include hundreds of events with intensity thresholds $I(\geqslant 10\ \text{MeV}) \geqslant 1.0$ pfu (proton flux unit: 1.0 pfu = 1 proton/cm s sr). Since 1976, the NOAA/USAF Space Environment Services Center, USA [61] has been publishing results of satellite observations (GOES program) for SPEs with threshold intensities $I(\geqslant 10\ \text{MeV}) \geqslant 10.0$ pfu.

As of February 2018, a total of 72 GLE type events had been officially registered (http://gle.oulu.fi) in the relativistic energy region during the entire observation period; the last one occurred on 10 September 2017. It can be thought that a number of weak GLEs escaped registration in the early years (before the creation of the worldwide network of CR stations) for technical and methodological reasons. Assuming their mean occurrence rate η to be $\sim 1.0\ \text{year}^{-1}$, a considerable number of events can be regarded as having been missed in 1942–1956 [62]. Recent developments in the theory of SCR acceleration by CME-driven shocks have attracted attention to weak GLEs. A new term, 'unidentified, hidden GLEs' [63] or sub-GLEs [64], was coined to define such events. They appear to include certain past weak events (remaining unexplored) and a number of those that occurred during the current cycle 24 of solar activity, e.g., the event from a post-limb source dated 6 January 2014. It was registered by several polar NMs at their detection limits. This event should probably be designated as GLE72.

Some proton 'superevents' observed from time to time in the nonrelativistic region (see monograph [20], Section 12.7.1) are characterized by a long duration (tens of days), with intensity of protons with $E \geqslant 10$ MeV varying but insignificantly as a function of heliolongitude. Elucidation of their relationship with other solar events [65] points to the fact that superevents are the strongest transient perturbations in the heliosphere. According to Ref. [65], superevents in the interplanetary space are always associated with the presence of fast CMEs reaching velocities in excess of 400 km s^{-1}. The authors of Ref [65] believe that this suggests an almost 100% relationship between such CMEs and individual SPEs [66].

Of special interest are so-called 'uncontrollable events' or 'rogue events' (see Ref. [20], Section 5.9), akin to solitary oceanic waves having unusually high amplitudes. In all probability, such events are related to particle acceleration at the fronts of multiple CME-driven shock waves in the interplanetary space. Well-known events of this kind are, in particular, the SPEs observed on 17 July 1959, 4 August 1972, 19 October 1989, and 14 July 2000 [67]. Similar events were registered on 12 November 1960 [68] and 12 October 1981 [69]. It can be speculated that particles were accelerated between the fronts of two approaching shock waves by means of the first-order Fermi mechanism, as suggested by the very steep SCR spectrum ([20], Fig. 9.4) derived from the NM data for the 04.08.1972 event. See also Refs [20, 29] for a brief discussion of such events observed in August 1972 and July 1959.

3. Mechanisms of acceleration, particle spectrum and composition

3.1 Pivotal problems of SCR physics

We distinguish two pivotal problems of SCR physics encompassing all other pertinent issues both being explored and pending solution. One is the shape of the spectrum in the context of the particle acceleration mechanism (model). Analogously, the other pivotal problem comprises the charge state and elemental composition of accelerated particles.

The spectrum of solar cosmic rays in major SPEs may span 4–5 orders of magnitude in energy: from ~ 1 MeV to $\gtrsim$10–100 GeV. The difference between intensities at the edges of the spectrum can be as large as 6–8 orders of magnitude due to its steepness in the high-energy region [38]. Hence, there are some technical and methodological difficulties involved in the measurement of SCR fluxes against the background of GCRs near Earth and in the interpretation of the data obtained. This is of special importance when it comes to validation of acceleration models. As a rule, to determine the shape of the spectrum in a wide energy range, results of several measurement options (on the Earth surface, in the stratosphere, aboard a spacecraft, etc.) need to be combined, which brings uncertainty into the resultant spectral characteristics. The key to the secrets of SCR spectrum formation at energies of $\leqslant 1$ MeV and $\geqslant 10$ GV appears to lie at the spectrum 'ends'.

In addition to energy units (eV, keV, MeV, GeV), CR researchers extensively utilize magnetic rigidity units $R = cp/Ze$ of particles (rigidity = momentum unit p per unit charge Z), usually expressed in volts, megavolts, and gigavolts. The energy–rigidity relationship is defined by formulas $E_\mathrm{k} + E_0 = [E_0^2 + (ZeR)^2]^{1/2}$ and $R = [E_\mathrm{k}^2 + 2E_\mathrm{k}E_0]^{1/2}$, where E_0 is the rest energy, and E_k is the particle's kinetic energy. Rigidity is convenient to use for the analysis of particle movements in a magnetic field B, because it is related by simple expressions to the Larmor frequency $\omega_B = ZeB/mc$, Larmor radius $\rho = v/\omega_B$, and magnetic field: $R = \rho B$ (m and v are the particle mass and velocity, respectively).

3.2 Spectrum shape

In the narrow energy ranges, SCR researchers widely rely on four main formulas for spectrum representation, viz. power and exponential functions of particle energy E or rigidity R:

$$D(E) = D_{01}E^{-\gamma}, \tag{1}$$

$$D(R) = D_{02}R^{-\gamma}, \tag{2}$$

$$D(R) = D_{03}\exp\left(-\frac{R}{R_0}\right), \tag{3}$$

$$D(E) = D_{04}\exp\left(-\frac{E}{E_0}\right). \tag{4}$$

Here, parameters D_{01}, D_{02}, D_{03}, and D_{04} are the respective normalizing coefficients, γ is the exponent, and R_0 and E_0 are the characteristic rigidity and energy of the differential spectrum, respectively. Parameters γ and R_0 are subject to changes, depending on the energy (rigidity) range being considered, and undergo temporal variations during an SPE. Sometimes, the above formulas are used in a modified version, e.g., as a combination of the power and exponential functions:

$$D(E) = D_{05}E^{-\gamma}\exp\left(-\frac{E}{E_\mathrm{c}}\right) \tag{5}$$

with a spectrum cut-off at energy E_c [70] or more complex combinations, such as a spectrum of two power functions with the break point at a given energy E_b. Their great variety reflects the mere fact that the conditions of SCR spectrum formation in a source (sources) within a wide energy range and allowance made for the transport effects in the IMF preclude its adequate description by simple relations (1)–(5).

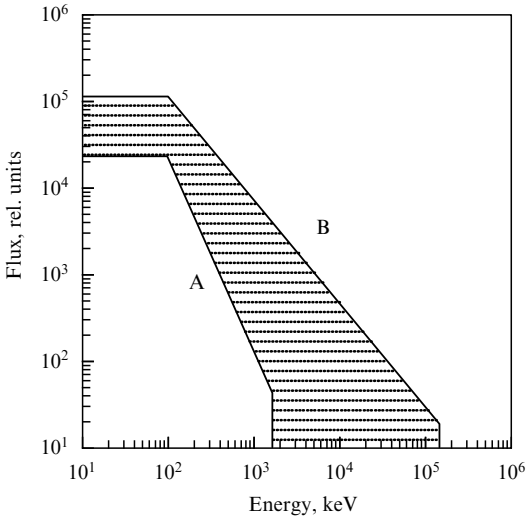

Figure 7. Spectrum of accelerated solar protons proposed in Ref. [71] to correlate observations in Earth's orbit and the assumption of acceleration of nonrelativistic protons in the coronal current sheet. Variations of spectral parameters in the shaded region can be accounted for by changes in CS parameters.

Hence, attempts have been made to empirically present the SCR spectrum based on observational data and/or proceeding from general physical considerations. Figure 7 schematically shows a spectrum in the energy range from 0.01 MeV to 1 GeV [71] proposed to describe selected observations (mostly for the nonrelativistic region). Spectrum A describes particle distribution in small-scale events, and spectrum B particles accelerated in a powerful flare in the coronal current sheet (CS). According to the authors of Ref. [71], variations of the spectrum within the shaded region reflect changes in the CS size and other parameters. In practice, it is very difficult to obtain a real spectrum of accelerated particles in a source [20]. Shock waves in the corona and effects of accelerated particle transport in the IMF arising from particle speed dispersion considerably modify the spectrum. As a result, SPE spectra near Earth are characterized by a large variety of shapes and intensities. Only the spectrum of particles with energy $E \geqslant 500$ MeV approximately corresponds to the source spectrum. However, even such particles experience the influence of transport effects. Variability of the spectrum shape and its 'droop' in the relativistic region are the basic characteristics of SCRs, and any acceleration theory claiming to be complete must be able to explain them.

In contrast to the schematic spectrum in Fig. 7, here are the spectra of several real SPEs examined in a series of publications [72–74]. Figure 8a depicts the 'instantaneous'

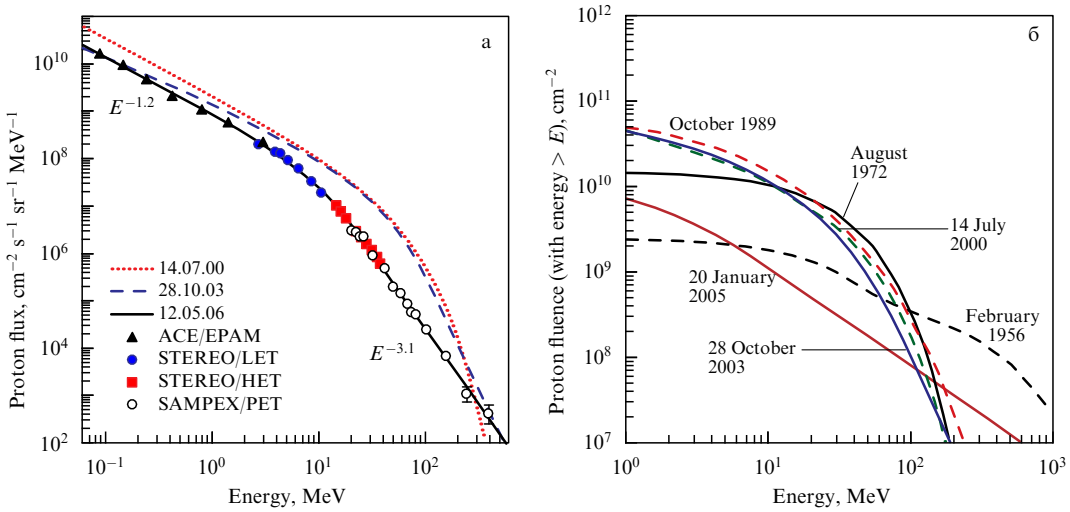

Figure 8. (Color online.) (a) Differential spectra for several SPEs measured in Earth's orbit (14 July 2000; 28 October 2003; 12 May 2006) and some distance away from Earth (5 December 2006). (b) Proton fluence spectra for several massive events of 1956–2005 (adapted from Refs [72–74]).

differential spectra for three events measured in different energy ranges near Earth's orbit. For comparison, the data obtained by three spacecraft for the event of 5 December 2006 are shown. These latter measurements were made far from Earth (by the ACE spacecraft at the Lagrangian point L1).

Figure 8b demonstrates integral energy spectra of the so-called fluences (fluence is a flux of protons integrated over the entire duration of a given event) for several remarkable SPEs. This SPE characteristic is of importance in the first place for the study of SCR geophysical effects, e.g., for the calculation of the cosmogenic isotope generation rate in Earth's atmosphere (see Section 8.2) and the evaluation of radiation hazard near Earth's orbit.

Marked differences are well apparent between events as regards the form of their spectra and the magnitude of fluence in each event. The spectra have a pronounced variable slope that becomes steeper with a rise in energy; in other words, the exponent γ depends on the energy. The cause of such behavior is thus far unknown. One can only state that a spectrum above the break energy might be described by a power function with an exponential cut-off [55]. According to Ref. [74], such spectra are better described by the specific double power function proposed by the authors of paper [75].

The following Sections 3.3 and 3.4 are focused on the relativistic part of the SCR spectrum where, in our opinion, the key to understanding mechanisms of particle acceleration and the maximum potential of the solar accelerator (accelerators) lies.

3.3 Maximum SCR energy

One of the most important characteristics of the solar accelerator (or accelerators?) is the maximum SCR energy. We mentioned in Section 2.2 the attempts to detect (measure) a limiting energy E_m that may be provided by the Sun's particle accelerator. Specifically, outbursts of secondary muon intensity at a water equivalent depth of ~ 200 m were recorded [39] with the effective energy of primary particles exceeding approximately 100 GeV. The outbursts correlated with solar flares, but their intensity did not exceed 3σ.

Later research with the Baksan Underground Scintillation Telescope (BUST) (Baksan Neutrino Observatory, Institute for Nuclear Research of the Russian Academy of Sciences) confidently demonstrated the so-called Baksan effect, i.e., statistically significant [39] short-lived bursts of muon intensity with an amplitude of up to 5.5σ and threshold energy $E_\mu \geqslant 200$ GeV corresponding to the primary proton energy $E_p \geqslant 500$ GeV. The outbursts fairly well correlated with GLEs. By the end of 2005, the inventory of muon outbursts recorded by BUST listed as many as 34 events [76]. These findings gave a novel impetus to the search for the SCR upper energy limit based on the results obtained by nonstandard CR detectors in many laboratories around the world. In what follows, some recent results of different authors are presented with special reference to the most striking GLEs of the 23rd solar cycle, such as those recorded on 6 November 1997 (GLE55), 14 July 2000 (GLE59), 15 April 2001 (GLE60), 28 October 2003 (GLE65), and 20 January 2005 (GLE69).

3.4 SCR upper limit spectrum

Generalization of the available data on maximum SCR fluxes made it possible to build up an empirical model of the integral SCR 'limit' spectrum in a broad energy range, at least between $E_p \geqslant 1$ Mev and $E_p \geqslant 10$ GeV [41]. The spectrum was constructed making use of maximum proton intensities $I_p(t_m)$ at the instant of maximum t_m near Earth (the so-called time-of-maximum (TOM) method) (see paper [15] for details). The spectrum can be approximated by several power functions with exponents depending on the chosen proton energy range: $\gamma = \gamma_0 E^a$, where $a = 1.0$ for $E_p \geqslant 1$ MeV [16]. In the English-language literature, the term upper limit spectrum (ULS) has been adopted. ULS parameters are presented in Table 1 with $I_p(t_m)$ values expressed in pfu.

The problem of SCR limit energy and upper limit spectrum was of primary interest in many publications. Specifically, the author of Ref. [78] attempted to implement

Table 1. Parameters of SCR upper limit spectrum.

E_p, eV	$> 10^6$	$> 10^7$	$> 10^8$	$> 10^9$	$> 10^{10}$	$> 10^{11}$
Index γ	1.0	1.45	1.65	2.2	3.6	> 4.0
$I(> E_p)$, pfu	10^7	10^6	3.5×10^4	8×10^2	1.2×10^0	7×10^{-4}

the general physical approach taking account of an obvious restriction, namely the existence of natural physical bounds for spectral parameters on the Sun. As is well known, the highest SCR intensities observed in the interplanetary space correspond in the first approximation to the source spectrum (see a preceding paragraph mentioning the TOM method). To characterize the SCR upper limit spectrum near Earth, the author of Ref. [78] made use of the source spectrum deduced in Ref. [79] from general principles of thermodynamics, regardless of concrete parameters of acceleration mechanisms (emissivity of SCR 'gas' particles, i.e., their escape from the shrinking trap). In this case, the differential distribution of SCRs over energies is a power function with exponent -3.5 or -5.0 for the nonrelativistic and ultrarelativistic 'gases', respectively. The author of Ref. [78] normalized spectrum [79] to GCR intensity at the maximum energy of solar protons, assumed to be roughly 20 GeV (which is far from recent estimates; see arguments in Section 3.5).

Figure 9 compares 'empirical' [16, 41, 77] and 'physical' [78] SCR spectra. Marked differences between them are manifested at the lowest and highest energies: the spectrum in Refs [41, 77] gives higher intensity values for $E_p \leqslant 50$ MeV and $E_p \geqslant 1$ GeV than in Ref. [78]. The cause behind this discrepancy remains unclear and awaits further studies to be elucidated.

Despite limited experimental resources, methodical difficulties, a paucity of observational data, and theoretical complexity, the problem remains a subject of inexhaustible interest by virtue of its fundamental character. For a comparison with observations, here are results of an analysis of the data obtained with the aid of the high-energy muon spectrometer of the "L3 + C experiment" (CERN) [80] during GLE59 or the Bastille Day Event (BDE), mentioned in Section 2.6 in connection with 'rogue events'. The study revealed a 5.7σ-muon excess, while the duration of the effect coincided with the period during which a peak flux of lower energy protons, X-rays and gamma radiation were observed.

Monte Carlo simulation [80] showed that the muon outburst was caused by primary protons with energy $E_p > 40$ GeV (most likely ~ 82 GeV). The results of simulations allowed the upper limit of such proton flux to be estimated as $\sim 2.5 \times 10^{-3}$ pfu. Notice that this value is much higher than the spectrum level in Refs [78, 79] that characterizes the source spectrum in the relativistic region but matches the upper limit spectrum [47, 77] for $E_p \geqslant 80$ GeV (Fig. 9). According to Ref. [80], the high-energy protons were accelerated during the impulsive phase of the 14 July 2000 flare 2 minutes after the onset of outbursts of hard X-rays and gamma radiation.

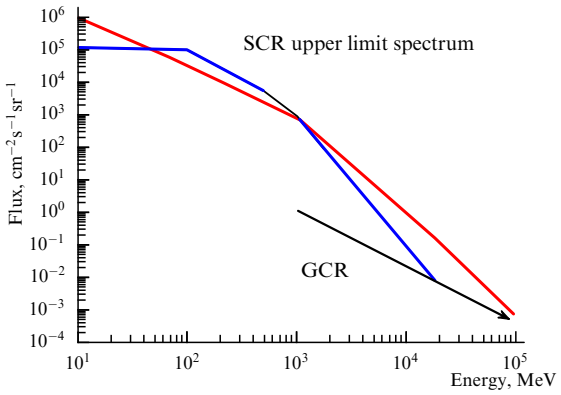

Figure 9. (Color online.) Comparison of two models of the integral SCR upper limit spectrum. Red color denotes the 'empirical' spectrum [41, 77], blue is the 'physical' spectrum [78]. The black straight line at the bottom indicates the integral GCR upper limit spectrum in the region of energies $\geqslant 1$ GeV. Estimates from report [78] were normalized to the GCR flux at $E = 20$ GeV, assumed to be maximum for SCR [78].

3.5 Data from nonstandard detectors

Apart from expanding total muon outburst statistics in BUST research ('Baksan effect'), the authors of report [76] made some progress in understanding this phenomenon. Specifically, they re-evaluated the maximum intensity of primary protons responsible for the muon outburst of 29 September 1989 (GLE42) with an amplitude of around 5.5σ. The outburst was estimated at $I_p(\geqslant 500\ \text{GeV}) \approx (1.5 \pm 0.2) \times 10^{-6}$ pfu. This value appeared to fairly well correspond to the spectrum of the fast SCR component for this event [35]. Anyway, this estimate is consistent with $I_p(> 82\ \text{GeV}) \approx 2.5 \times 10^{-3}$ pfu for the BDE [80].

Thus, data from nonstandard detectors obtained during GLEs provide very important information about the upper bounds of solar proton fluxes in the relativistic region and maximum SCR energy. Despite being fragmentary and not amenable to consistent interpretation, these data raise questions of crucial importance, e.g., whether particles in the Sun are really accelerated up to $E_p \geqslant 500$ GeV or we are dealing with some specific effects of GCR modulation. These questions were raised before only in respect to individual GLEs.

The theory of acceleration cannot thus far offer an adequate description of the total SCR spectrum, especially for $E_p \geqslant 100$ GeV, even if there are very simple estimates of the maximum energy [81] based on the coronal CS model. For example, the value of $E_m \approx 250$ GeV was obtained for the event of 23 February 1956 (GLE05) — the strongest single one in the relativistic energy region. At the same time, observations of such events as those dated 23 February 1956, 29 September 1989, 6 November 1997, and 15 April 2001 using nonstandard detectors gave conclusive evidence of solar protons with energies $E_p \geqslant 10$ GeV (and even $\geqslant 100$ GeV). However, there are still few detectors capable of recording secondary muons from such protons. To recall, information on anisotropy of incoming particles can be obtained only by single point measurements, which are not easy but are possible to make. At present, however, there are no muon detectors capable of measuring SCR anisotropy in GLEs. Therefore, the authors of Ref. [15] reasonably believe that several ground or underground muon detectors sufficiently sensitive in different directions could substantially improve performance of the worldwide network of NM stations.

4. New GLE concept

4.1 GLE sources: a flare and/or CME?

Key questions about the nature of GLE, SCR sources and acceleration mechanisms have been the focus of attention for a few decades. Especially intriguing is the 'flare or CME dilemma' (see Fig. 3). Its discussion is centered on which of the active solar processes — flare, coronal mass ejection, or both — is responsible for SCR generation. It appears there can be no straightforward answer to this question, whereas relevant indirect evidence *pro* and *con* is far from being reconciled. In light of modern views of the essence of the

problem, it can only be stated that the eruptive character of energy liberation in the solar atmosphere implies rapid acceleration of particles up to high energies.

To begin with, this inference is consistent with GLE observations. For example, even in the relatively weak GLE71 of 17 May 2012 (see Fig. 4), neutron monitors recorded a growth in intensity within a few minutes, whereas its reduction took hours. On the other hand, rapid acceleration is in excellent agreement with the theoretical model of relativistic particle generation in flares proper; it is a well substantiated and physically transparent concept [82–88] of magnetic field reconnection in the solar corona. Its development and first applications date back to the early 1960s (see Refs [84–86] and references cited therein); it was finally recognized in Refs [87, 88].

It became clear by the early 1960s that the source of the huge energy released in solar flares was the energy of magnetic fields associated with electric currents flowing in the corona. S I Syrovatskii, the author of the pioneering study [82], considered the general nonstationary problem of compressible plasma flows in a nonuniform two-dimensional magnetic field with the zero line. As a result, a fundamental conclusion was reached that highly conducting plasma flows in this field are responsible for the strong concentration of magnetic energy and the formation of a current sheet separating oppositely directed fields [82, 83]. Liberation of the magnetic energy concentrated in the vicinity of the CS is possible only in the case of its rapid breakdown, which, in turn, facilitates the generation of strong electric fields accelerating charged particles. According to the concept framed in Refs [82, 83], the cumulation of magnetic energy and CS formation are inevitable attributes of the pre-flare situation. The flare proper occurs upon CS breakdown, when the energy cumulated due to magnetic reconnection is converted into the thermal and kinetic energy of the plasma, the energy of accelerated particles (SCRs), and radiation energy in different ranges of the electromagnetic spectrum.

Thus, Syrovatskii [82, 83] appears to have been the first to come up with the idea of the 'cumulative' mechanism of acceleration realized during a solar flare. This mechanism accelerates all particles, regardless of their properties, in a distinguished relatively small region of the plasma. In other words, acceleration is spatially nonuniform. Such a mechanism is essentially different from statistical acceleration mechanisms governing acceleration of a small portion of the particles differing from the remaining ones in certain parameters, e.g., initial energy, mass, or charge. The author of papers [82, 83] emphasized the very general character of "the process of rapid dissipation of the magnetic field accompanied by the appearance of high-energy particles", quite apparent not only in solar flares but also in many other phenomena inherent in both cosmic and laboratory plasmas, as was soon confirmed in experiment (see, for instance, review [86] and the reference cited therein).

In recent years, the magnetic reconnection concept with regard to SCR acceleration has been addressed both theoretically [87] and in terms of numerical simulation supplemented by comparison with observational data (see Section 4.3 below). By way of example, the authors of Ref. [89] considered the analytical solution of the relativistic equation of motion for charged particles in a reconnecting CS with the three-component magnetic field ($B_0 \approx 100$ Gs, $B_{||} \approx 0.1B_0$, $B_\perp \approx 5 \times 10^{-4} B_0$) and strong electric field E_a (up to ~ 30 V cm^{-1}) resulting from magnetic reconnection. Particles are accelerated along the electric field practically up to the speed of light, and their kinetic energy is proportional to the time they spend within the sheet. The numerical solution of the equation for the above parameters B and E_a suggests that electrons can be accelerated for $2 \times 10^{-7} - 10^{-3}$ s in a region $\sim 7 \times 10^2 - 3 \times 10^7$ cm in size; the analogous values for protons are $10^{-4} - 2 \times 10^{-2}$ s and $\sim 3 \times 10^5 - 7 \times 10^8$ cm, respectively. Various aspects of the magnetic reconnection concept, including particle acceleration under astrophysical conditions, are highlighted in a special monograph [88], where the authors pay tribute to the contribution made by Soviet (Russian) scientists.

4.2 Two relativistic components of GLE

As shown in Ref. [90], GLEs account for roughly 15% of all major SPEs ($\geqslant 10$ pfu) that occur during a cycle of solar activity. Hence, a natural question: what should the specific conditions on the Sun be to ensure generation of GLE? Let us consider the problem in more detail, taking account of the available observational data and their possible interpretation.

There is currently a wealth of evidence in favor of the assumption that in many GLEs a flux of relativistic SCR not infrequently consists of two components, prompt (PC) and delayed (DC). According to Refs [16, 20], the PC is in all likelihood associated with a flare, and DC with CME [91]. On the other hand, some authors advocate the conjecture that CME-driven shock waves are the sole accelerators of solar energetic particles (SEPs) [13], right up to GLE particles [92]. One of the arguments in favor of this assumption is the characteristics of SEPs (mostly protons having energies exceeding 10 MeV) with energies by 1–2 orders of magnitude lower than in GLE cases). Adherents of this opinion also refer to the data on solar radio, X-ray, and gamma radiation, measured SEP elemental compositions and spectra, etc.

All these observations are compared, in one way or another, with flare and/or CME characteristics. Meanwhile, it has been shown that the appearance of SEPs in Earth's orbit is a result of a series of preceding physical processes (sometimes of unknown origin). Spectra, time profiles of intensity and other characteristics of SEPs observed near Earth experience the influence of multiple and/or long-term acceleration in the source [93] and/or their propagation in the interplanetary medium [20, 94].

The authors of Ref. [95] used a generally accepted method to analyze SCR ground level enhancements [16] in order to examine 35 major GLEs recorded during 1956–2006. Optimization techniques were employed to solve the reverse problem; specifically, the SCR spectrum in Earth's orbit was reconstructed in absolute units based on the data of the worldwide system of stations. Each GLE with rare exception was found to consist of two relativistic components: an PC with the exponential spectrum (4), and a DC with a power-law spectrum (1). It should be noted that the shape of the spectra was not explicitly given to measure their parameters on the rigidity scale. The shape of the spectra obtained after solving the reverse problem was determined from the perfect agreement with one of the two representations, either exponential or power law. Table 2 collates spectral parameters of 35 events, with D_{04} and D_{01} having dimensions m^{-2} s^{-1} sr^{-1}GeV^{-1}, and E and E_0 having GeV. Mean values deduced from these data are $\langle E_0 \rangle = 0.52 \pm 0.15$ GeV, and $\langle \gamma \rangle = 4.8 \pm 0.25$. Notice that the temporal separation of SCR fluxes into the PC and DC, as well as the examination of other fine details of individual ground enhancements, became

Table 2. Spectra of two SCR components in GLEs 1956–2006 [95].

GLE No.	Date of flare	Radio II type UT	Flare class	Flare location	Spectrum parameters			
					PC		DC	
					D_{04}	E_0	D_{01}	γ
05	23.02.1956	03:36	3	N23 W80	7.4×10^5	1.37	5.5×10^5	4.6
08	04.05.1960	10:17	3+	N13 W90	2.7×10^5	0.65	1.6×10^3	4.2
10	12.11.1960	13:26	3+	N27 W04	—	—	7.5×10^3	4.1
11	15.11.1960	02:22	3	N25 W35	—	—	1.0×10^5	5.3
13	18.07.1961	09:47	3+	S07 W59	5.2×10^3	0.52	3.6×10^3	6.0
16	28.01.1967	07:55	—	N22 W154	1.4×10^4	0.58	6.7×10^3	4.7
19	18.11.1968	10:26	1B	N21 W87	1.2×10^4	0.58	2.6×10^3	5.5
20	25.02.1969	09:04	2B/–	N13 W37	7.7×10^4	0.38	4.7×10^3	5.0
22	24.01.1971	23:16	3B	N19 W49	3.4×10^4	0.45	8.7×10^3	5.8
23	01.09.1971	19:34	—	S11 W120	—	—	4.7×10^3	5.4
25	07.08.1972	15:19	3B	N14 W37	6.6×10^2	1.23	4.3×10^2	5.0
29	24.09.1977	05:55	—	N10 W120	6.5×10^2	1.14	9.3×10^2	3.2
30	22.11.1977	09:59	2B	N24 W40	1.5×10^4	0.77	1.1×10^4	4.7
31	07.05.1978	03:27	1B/X2	N23 W82	3.5×10^4	1.11	1.3×10^4	4.0
32	23.09.1978	09:58	3B/X1	N35 W50	—	—	7.0×10^2	4.7
36	12.10.1981	06:24	2B/X3	S18 E31	1.7×10^3	1.21	—	—
38	07.12.1982	23:44	1B/X2.8	S19 W86	5.7×10^3	0.65	7.2×10^3	4.5
39	16.02.1984	09:00	—	– W132	—	—	5.2×10^4	5.9
41	16.08.1989	01:03	2N/X12.5	S15 W85	6.8×10^3	0.56	3.8×10^3	5.1
42	29.09.1989	11:33	–/X9.8	– W105	1.5×10^4	1.74	2.5×10^4	4.1
43	19.10.1989	12:49	3B/X13	S25 E09	4.0×10^4	0.53	3.0×10^4	4.8
44	22.10.1989	17:44	2B/X2.9	S27 W31	7.5×10^4	0.91	1.5×10^4	6.1
45	24.10.1989	18:00	2B/X5.7	S20 W57	2.4×10^4	0.72	1.1×10^5	4.9
47	21.05.1990	22:12	2B/X5.5	N35 W36	6.3×10^3	1.13	2.7×10^3	4.3
48	24.05.1990	21:00	1B/X9.3	N36 W76	2.8×10^4	0.60	9.1×10^3	4.3
51	11.06.1991	02:05	2B/X12.5	N32 W15	2.6×10^3	0.83	3.3×10^3	4.8
52	15.06.1991	08:14	3B/X12.5	N36 W70	—	—	5.8×10^3	4.6
55	06.11.1997	11:53	2B/X9.4	S18 W63	8.3×10^3	0.92	8.2×10^3	4.6
59	14.07.2000	10:19	3B/X5.7	N22 W07	3.3×10^5	0.50	5.0×10^4	5.4
60	15.04.2001	13:48	2B/X14.4	S20 W85	1.3×10^5	0.62	3.5×10^4	5.3
61	18.04.2001	02:17	—	– W120	2.5×10^4	0.52	1.2×10^3	3.6
65	28.10.2003	11:02	4B/X17.2	S16 E08	1.2×10^4	0.60	1.5×10^4	4.4
67	02.11.2003	17:14	2B/X8.3	S14 W56	4.6×10^4	0.51	9.7×10^3	6.3
69	20.01.2005	06:44	2B/X7.1	N14 W61	2.5×10^6	0.49	7.2×10^4	5.6
70	13.12.2006	02:51	2B/X3.4	S06 W24	3.5×10^4	0.59	4.3×10^4	5.7

possible only by virtue of the high accuracy of GLE recording by SNM-64 neutron supermonitors [35].

It is convenient to demonstrate the properties of two-component GLEs as exemplified by the event of 29 September 1989 (GLE42) [38]. It proved to be the most remarkable one for the entire period of SCR observations [20]. The event was associated with a powerful behind-the-limb source (a $\geqslant$ X9.8 flare) and accompanied by rapid CME (radial velocity of 1828 km s^{-1}); according to data from the NM network, it was characterized by a well-expressed and very complicated time profile of intensity, as illustrated in Fig. 10a. Our analysis showed that high-cutoff rigidity stations, e.g., Alma-Ata, recorded only the PC with a very hard spectrum (first injection). Other stations observed a mixed picture. For

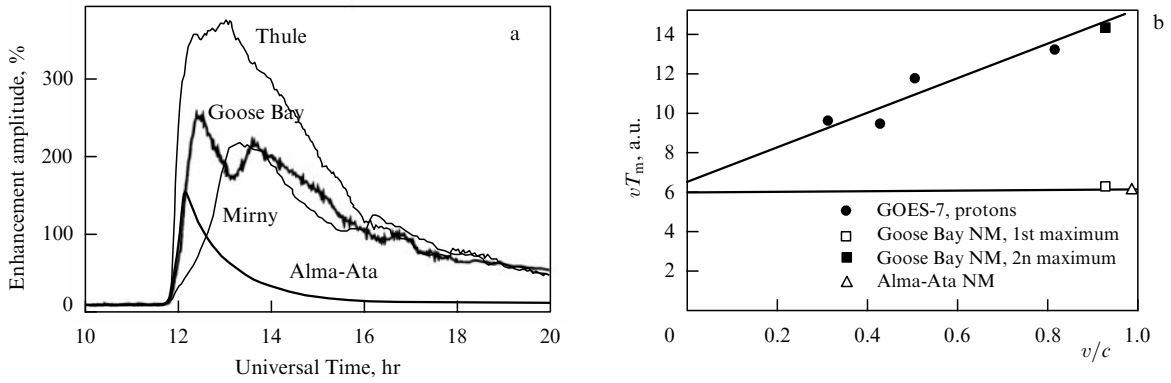

Figure 10. (a) SCR intensity-time profile of the 29.09.1989 event (GLE 42) based on the data from four NM stations with different cutoff rigidities R_c: Alma-Ata (6.61 GV), Mirny (0.03 GV), Goose Bay (0.64 GV), and Thule (0.00 GV). (b) Separation of two relativistic components in the same event by the vT_m method [97]; horizontal axis is the relative speed of particles in fractions of the speed of light.

example, the data from the Mirny station (Antarctica) gave evidence of a second (delayed) injection (DC) with a softer spectrum. The high-latitude Goose Bay station (Canada) registered an intensity profile exhibiting two pronounced peaks of about 1 hour apart.

The first peak was most probably produced by the prompt component, since it is synchronized with the Alma-Ata profile, whereas the second one appears to be related to the second injection, because it coincides with the delayed Mirny profile. A rather flat maximum recorded by the Thule station (Greenland) appears to have formed as a result of the overlap of the fast and delayed components. The possible disposition geometry of two sources and the general scenario were described for the first time on the assumption of two sources of relativistic protons already near the Sun [96].

The division of GLEs into two components is substantiated with the use of a simple TOM-method: multiplication of particle velocity v by the time T_m of the particle intensity maximum near Earth gives the distance $S = vT_m$ covered by the particles in the interplanetary space after injection (Fig. 10b). Direct measurements of the injection instant of time being absent, the authors of Ref. [97] related the onset of emission of accelerated particles to the moment of a type II radio burst. They used for analysis not only data from ground-based neutron monitors but also the results of measurements of SCR fluxes by the GOES-7 satellite in four energy ranges.

Figure 10b shows that observational data give evidence of two linear dependences. The steeper dependence integrates measurements of nonrelativistic protons by the GOES-7 spacecraft with the second Goose Bay intensity maximum. All these particles appear to have belonged to one DC population detained in the corona. The second straight line is drawn through the points corresponding to the intensity maximum at the Alma-Ata station (PC) and the first Goose Bay maximum, which means that the PC contained only relativistic particles that left the source without delay.

4.3 The nature of fast and delayed component sources

It follows from the foregoing that all significant GLEs, i.e., events with a perfectly developed time profile, have a well-defined two-component structure exhibiting first a PC, then a delayed component. In the 'classical' case of CLE42 (29 September 1989), the time interval between the PC and DC maxima was $\sim$ 1 hour [38]. Observations of PCs and DCs showed that they differ in the following three main characteristics: (1) the shape of intensity–time profiles (impulsive and gradual), (2) pitch-angle distributions (anisotropic and near-isotropic), and (3) the shape of the energy spectra (hard exponential and soft power-law). At the onset of GLE, the PC is, among other factors, highly anisotropic; its particles are believed to be accelerated in the magnetic reconnection processes in the lower coronal layers at a moment close to the flare eruptive phase and the beginning of type II radio outburst indicative of the formation of a shock wave in the corona and CME generation. DC particles can be accelerated [91] by the stochastic mechanism in closed magnetic structures over the reconnection region. Thereafter, they are expelled into the outer corona as CME expands.

The first attempts to adequately interpret the spectra of two SCR components in physical (model) terms taking into consideration the nature of their solar sources date to the early 1990s [81, 91, 98]. It was shown that acceleration in the electric field generated by magnetic reconnection in the coronal CSs is the most feasible mechanism for the PC formation. As a result, the spectrum of accelerated protons acquires an exponential shape resembling $\sim \exp(-E/E_0)$. For the event of 14 July 2000 [98], the characteristic energy E_0 of the spectrum proved, in particular, to be equal to 0.51 GeV, i.e., close to the mean E_0 value for the majority of the events listed in Table 2.

The stochastic mechanism underlying turbulence-driven acceleration in the perturbed plasma of a flare surge or coronal ejection has been regarded as the most probable source of DCs [91]. Another possible mechanism, in accordance with model [70], is the simultaneous acceleration of electrons, protons, and alpha-particles by a shock wave in the solar corona. This mechanism seems to be efficient but only in the nonrelativistic energy region. The main argument against shock wave-driven acceleration of SCR particles up to relativistic energies is that this mechanism produces a hard power-law spectrum with differential index $\gamma = 2.0-2.5$ [99], whereas the DC spectrum has the mean index $\gamma \approx 5$ (according to ground-based observations). Just such an index was obtained in the model of stochastic acceleration by plasma turbulence [91].

4.4 Acceleration by shock waves

The mechanism of superadiabatic acceleration by a shock wave was proposed in the late 1970s [99], largely to account for the spectrum shape of GCRs believed to be produced by

supernova explosions (flares). The first application to the SCR problem was study [70] dealing with a simplified (linear) variant of the first-order Fermi acceleration ('diffusive' acceleration [99]) at a shock wave. Based on certain simplifying assumptions, the authors of paper [70] obtained expression (5) for the description of SCR spectra that they considered to be suitable for the characteristics of both electron spectra starting from 100 keV and GLE proton spectra up to 10 GeV. However, this mechanism is of limited application as regards GLE generation, i.e., acceleration in the solar corona and the interplanetary medium [15]. Its realization requires, inter alia, the so-called 'injection energy', i.e., preliminary acceleration. Moreover, some earlier estimates [100] suggest that this mechanism cannot accelerate particles to a maximum energy higher than 1 GeV. The further development of the theory of this mechanism contributed to a better understanding of its details, physics, methods of simulation, and validation based on experimental data. A special term, 'diffusive shock acceleration (DSA)', was coined, meaning that acceleration occurs at plasma irregularities (wave turbulence) near the shock wave front. The energy of accelerated particles comes from the shock wave energy, while turbulence before and behind the front keeps particles near the front until they escape away.

We are of the opinion that the authors of Refs [101, 102] managed to develop the most detailed and consistent approach to the problem in both the linear [101] and nonlinear [102] variants of the theory. Based on modern semiempirical data on the plasma density altitude profile and the level and spectrum of Alfvén turbulence in the corona, they obtained the following formula for the SCR spectrum:

$$N(E) = N_0 E^{-\gamma} \exp\left[-\left(\frac{E}{E_{\max}}\right)^{\alpha}\right]. \qquad (6)$$

Here, N_0 is the normalization factor, and $E_{\max}$ is the characteristic spectrum energy. This expression contains a power-law part with index $\gamma \approx 2$ (comparable to the estimate in Ref. [70] for the shock wave) and the exponential 'tail' with parameter $\alpha \approx 2.3 - \beta$, where β is the exponent in the coronal Alfvén wave spectrum.

It follows from Refs [101,102] that $E_{\max}$ can vary in a wide 1–300 MeV range, depending on the shock wave velocity. The authors of Refs [101, 102] showed, based on an analysis of several SPEs, that formula (6) fairly well describes the SCR spectrum in the nonrelativistic region, but seems unsuitable to describe the relativistic region of the spectrum. At any rate, the model yields rather ambiguous results substantially dependent on the Alfvén turbulence spectrum index $\beta = 0.5-1.5$ as mentioned earlier in Ref. [15], when used to describe the spectrum above 1 GeV for GLE42 at the late isotropic stage of the event registered on 29 September 1989 (in fact, the DC spectrum alone). The authors of Refs [101, 102] did not consider at all the prompt component well manifested in GLE42 [35]. We undertook a critical analysis of the approach described in paper [101] in an earlier publication [15].

One of the last studies in this area [13] dealing with the large GLE65 of 28 October 2003 does not also give a satisfactory answer to all the questions concerning the formation of SCR spectra. Reames [13] considered only the delayed component of SCRs recorded at 14:00 UT during the isotropic stage of the event. The obtained SCR spectrum can be approximated with an acceptable accuracy by the function $D(E) = 350E^{-1.4} \exp(-E/450)\ \mathrm{cm^{-2}\,s^{-1}\,sr^{-1}\,MeV^{-1}}$. Importantly, there is a bump in the 4–80 MeV region of the spectrum. The nature of such features frequently observed during acceleration at shock wave fronts under various astrophysical conditions has been discussed in many earlier publications. Yet, the problem remains to be clarified.

Among the attractive results of Refs [101–103] is a self-consistent scenario of particle acceleration, starting with shock wave generation in the corona to the formation of the SCR spectrum, with the completion of the process inside a distance of a few solar radii. For example, acceleration in GLE65 terminated at a height of up to $4R_S$ [103], i.e., beneath the solar wind outflow region on the Sun's surface. This does not contradict the estimated height of shock wave origination and CME formation in Refs [101, 102]. On the other hand, it is worth noting that strong anisotropy at the beginning of GLE suggests an ejection of relativistic particles from a point source like a solar flare rather than from a longitudinally extended source, such as a shock wave.

4.5 Role of interplanetary transport

The hypothesis of two components in relativistic SCRs put forward in the late 1980s was discussed in the literature from different perspectives over the following two decades (see papers [15, 16] and references cited therein for details). For example, the authors of Ref. [106] emphasized that the 'double structure' of intensity–time profiles in certain GLEs manifested itself not only in the 22nd SA cycle but also in cycles 19–21, e.g., in GLE11 of 15 November 1960) and, possibly, GLE25 (7 August 1972). The majority of such structures were observed at polar stations with narrow asymptotic acceptance cones facing the first arriving solar particles. In any case, the initial 'coherent spike' of intensity of relativistic solar protons at the beginning of a GLE can be a more common phenomenon than previously thought. By way of example, Ref. [107] presented evidence of two separate injections of relativistic solar protons some 10–20 min apart in the event of 22 October 1989 (GLE44).

In this context, results of satellite measurements of the same event are of special interest [108]. The authors analyzed intensity–time profiles of protons obtained by two geostationary satellites, depending on proton energy. They found that the 'peak' pronounced in the nonrelativistic region according to NM data could also be followed by energies up to $E_p \approx 15$ MeV. At the same time, a detailed analysis of GOES-7 data for the event of 29 September 1989 failed to reveal an analogous picture [35]. GOES-7 detectors registered the event in several low-energy channels, but all the channels registered only a smoothed time profile with a single peak. The intensity began to rise sharply earlier 12:00 UT and gradually reached the maximum value. The peak was registered after 13:00 UT, depending on particle energy in a given channel. Noteworthily, none of the low-energy channels demonstrated any specific features of time profiles, although all of them measured particles with rigidities < 2 GV. Even the channel with the highest energies in the 640–850 MeV range (rigidity $R \approx 1.6$–2.3 GV) accessible to observation by NMs gave evidence of a gradual increase in a maximum value. This sole peak was recorded by GOES-7 when NMs registered the second peak. In other words, the first peak observed by NMs was due to protons with rigidity $R > 2.3$ GV. Had GOES-7 'looked' in a different (opposite) direction, such a conclusion would have been less striking. In the present case, it only points out that the GOES-7 position was not optimal for recording the first peak.

To sum up the discussion of the nature of the PC and DC, it is worthwhile to point out some theoretical research on the release and interplanetary propagation of relativistic solar particles. For example, it was shown in Ref. [109] based on the Boltzmann kinetic equation for particles with anisotropic initial distribution that amplitudes and time profiles observed during anisotropic GLEs will depend on the direction of asymptotic radiation acceptance cones of neutron monitors with respect to the direction of particle transport in the IMF. This approach was employed in Ref. [109] to examine GLE48 (24 May 1990), remarkable for its strong initial anisotropy and signs of double SCR injection (see Table 2). To describe these features, the authors of Ref. [109] assumed a prolonged particle energy-dependent injection in GLE48.

However, such an approach appears insufficient to account for the long time delay between the anisotropic peak registered by several ground stations and the smoothed isotropic maximum at other stations, unless allowance is made for the possibility of a second SCR injection. To recall, a rapid increase in intensity (strong anisotropy) at the onset of an event suggests the possibility of direct access to the lines of force connecting the Sun and Earth for relativistic solar protons and their transport along the IMF practically without scattering. This means that interplanetary propagation cannot significantly change the spectrum of relativistic protons. In other words, we consider the above patterns and specifics of the two SCR components to be a consequence of the acceleration processes in the Sun.

4.6 Problem of first GLE particles

The explosive release of solar energy produces a flare and coronal mass ejection (CME). It is generally accepted that X-ray and gamma radiation are associated with solar flares. Radio emission is a sign of perturbations and particles propagating through the corona and interplanetary space. The particles can gain energy both in flares and the accompanying wave and shock processes, e.g., in shock waves associated with the reconnecting current sheet (see Ref. [87], Part II, Ch. 3). It is therefore difficult to distinguish signs of acceleration mechanisms based on particle observations. On the other hand, it seems reasonable to assume that the early phase of GLE events is closest to the onset of acceleration and the interplanetary transport is of little consequence for the particles that are the first to arrive.

Extremely large events provide the best opportunity for studying the early phase due to the high signal-to-noise ratio, while relativistic solar protons are the most suitable candidates for addressing the particle acceleration problem, as exemplified by the pioneering paper [110]. It was continued by many other researchers [111–114], who showed in Refs [111, 112] that the first relativistic particles leave the Sun at a moment close to the maximum of hard X-ray and high-energy gamma radiation [115]. These forms of radiation are inherent in the explosive phase of a flare.

Unlike the first particles, the DC appears 10–30 min after the PC, just when the CME occurs, in the absence of any correlation between particle fluxes and CME characteristics. The developing CME is preceded by a shock wave (type II radio source) that is capable of accelerating particles and producing a power-law spectrum with index $\gamma \approx 2.5$. The DC spectrum has the index $\gamma \approx 5$ better corresponding to stochastic acceleration [91]. Particles captured in loop-like magnetic structures inside the expanding CME are accelerated as they interact with plasma turbulence. Adiabatic losses (adiabatic cooling, to be precise) in such a trap are negligible in comparison with the acceleration effect [91]. The particles are liberated when the CME reaches the upper part of the corona.

A quite unexpected aspect of the problem of first SCR particles has recently been disclosed [116] when analyzing SCR effects in the anti-coincidence shield (ACS) (BGO scintillation detector weighing 512 kg) intended to screen the SPI spectrometer aboard the INTEGRAL orbital astrophysical laboratory. As is known, the onset of ground level enhancement (GLE) detected by one of the worldwide network NMs is traditionally assumed to be the arrival time of relativistic protons. Ambiguity and inaccuracy in determining the instant of arrival of solar protons by NM data are due to the detector intrinsic background (statistical accuracy of detection) and variations of both the geomagnetic cut-off rigidity threshold and the direction of the acceptance cone for arriving particles.

The authors of Ref. [116] brought to notice the fact that the count rate in the ACS detector during certain GLEs increased much earlier than in ground-based neutron monitors. They described two events in which the SPI-ACS detector proved to be more efficient instrument for recording the onset of the SPE – GLE in Earth's orbit than the NM network (GLE68 of 17 January 2005 and GLE70 of 13 December 2006). These events were relatively weak in terms of enhancement amplitude, but the arrival of relativistic protons at Earth was significantly delayed with respect to the outburst of hard X-ray radiation, which suggested a later onset of proton acceleration. At the same time, a rise in the count rate in the SPI-ACS detector caused by the arrival of relativistic protons was apparent earlier than that and corresponded to SCR acceleration at the moment of the flare. This observation underscores the necessity of designing detectors of solar protons and cosmic electrons with a low intrinsic background. Such detectors are needed to measure low-intensity SCR fluxes (the 'hidden GLE problem'). Indeed, unlike the two aforementioned weak GLEs, in two other extremely large events (GLE65 of 28 October 2003 and GLE69 of 20 January 2005) the arrival of solar protons at the SPI-ACS detector coincided with the onset of anisotropic enhancement in the NM network, i.e., the protons arrived simultaneously with the prompt component of SCRs.

4.7 GLE and the composition of accelerated particles

As mentioned above, the elemental composition and the charge state of SEPs are two pivotal elements of the overall SCR problem. The distribution of SEPs in terms of chemical composition is determined wherein by the so-called first ionization potential (FIP) of 'impurity' elements (C, N, O, Fe, Mg, and many others), while the charge state depends largely on the altitude of the coronal region (i.e., matter density and temperature) in which acceleration and subsequent ionization of particles (ions) occur. Data on heavy ions with the atomic number $Z \geqslant 2$ with due regard for their charge-to-mass ratio (Q/A), ^{3}He/^{4}He, and Fe/C or Fe/O ratios are widely used to investigate several complicated processes associated with the injection, escape, and transport of accelerated solar particles (SEPs).

It was proposed more than 25 years ago (see paper [51] and references cited therein) to differentiate solar flares and SEP fluxes generated by them into two classes: impulsive and gradual. The class of a flare and the related SPE can be identified based on a number of parameters. At present, the

division of flares and particle fluxes into two categories is considered to be a simplification [117], because certain events of different classes have some common features. Cane et al. [118] proposed to use the Fe/O ratio as the main characteristic for categorizing events into two different classes when comparing particle fluxes from impulsive and gradual flares.

On the other hand, the Fe/O ratio is a measure of the so-called FIP effect. The essence of the latter is as follows. The elemental composition of the photosphere as determined spectroscopically is highly homogeneous over the entire surface of the Sun. However, the content of impurity elements in coronal structures and in the solar wind shows a different FIP dependence with respect to their concentration in the photosphere.

By the mid-1980s, it was established [119] that fractionation of impurity elements on the basis of FIP is realized in the upper solar chromosphere. Low-FIP elements (< 10 eV — Fe, Mg, Si, K and others) are easily ionized and under the action of a pondermotive force from the side of Alfvén waves they are carried out to solar upper atmosphere [120] where these ions are able to accumulate in closed magnetic structures. On the other hand, the high-FIP elements (> 10 eV — C, N, O and others) remain there neutral and their content does not vary. Iron relates to elements with low first ionization potential and their concentrations in the solar upper atmosphere are increased several times. The content of oxygen there remains close to photospheric level, because its FIP exceeds 10 eV [121].

Results of Fe/O content measurements in accelerated particle fluxes from different flares have been reported in many earlier publications, but Fe/O ratios were determined only in one or two ion energy ranges, which proved insufficient to elucidate their energy dependence. Only papers containing statistically significant values are cited below. For example, the authors of Ref. [122] used the data of high-resolution mass spectrometers aboard the ACE to determine the event-averaged elemental composition within an energy range from ~ 0.1 to ~ 60 MeV/nucleon in 64 powerful SPEs of solar cycle 23. They showed that the Fe/O ratio either decreased or remained unaltered as the energy increased to ~ 60 MeV/nucleon in 64% of cases. This finding is consistent with the assumption that particles are accelerated at a shock wave from CME at a distance of 1 AU, the effect being a function of particle rigidity.

Taken together, this result and data on spectral breaks for different ions (see, for instance, Refs [123, 124]) suggest that acceleration at shock wave fronts is the dominant process in most major SPEs of the 23rd cycle of solar activity. However, the Fe/O ratio was shown to decrease at an energy of 310 MeV/nucleon in 36% of events. Such a behavior is actually surprising and may suggest a different acceleration mechanism operating at high energies, e.g., in events enriched in Fe ions [125]. It can be speculated that a 'seed' population of flare particles whose Fe/O ratio grows with energy undergoes additional acceleration [126]. Doubtless, alternative scenarios can also be relevant, but the available data are still insufficient to comprehensively address this issue.

Certain aspects of the problem have recently been considered in paper [127], where e/p and Fe/O ratios for several GLEs were compared with characteristics of the respective flares and CMEs on the assumption that GLEs represent an extreme case of gradual SEP events (SPEs) induced by shock waves from fast and extensive CMEs, which are, in turn, associated with long (> 1 h) outbursts of soft X-ray radiation. It turned out, however, that some large gradual SPEs, including GLEs, are related to shorter (< 1 h) flares. They are comparable to SPEs characterized by an increased content of heavy elements (e.g., a high Fe/O ratio), high degree of particle ionization (e.g., Fe ions), and large e/p ratio.

4.8 Composition of SCRs and properties of their sources

To understand how the e/p and Fe/O ratios measured in two energy ranges depend on characteristics of active regions, respective flares, and CMEs, Kahler et al. [127] undertook a statistical evaluation of 40 GLEs registered since 1976. It was revealed that the ratios of elemental contents tend toward lower and more stable values in the corona as the timescale (duration) of flares and peak fluxes of soft (thermal) and hard (bremsstrahlung) X-ray radiation increase together with the size of the active region.

The authors of Ref. [127] concluded that this result indicates that flare effects are insignificant in these GLEs if the wide region of 'heliolongitudes of coupling' between GLE sources with an increased content of heavier elements is taken into account. Moreover, the data [127] suggest that low-energy SEPs accompanying GLEs are mostly accelerated at the fronts of CME-driven shocks, and the relation of the flare power and time characteristics to the CME properties can explain the correlation between the SEP composition and the flare properties. This approach is consistent with the modern weighted view of the flare–CME dilemma (see Fig. 3).

However, it remains unclear, even on the assumption that the main contribution to GLEs comes from flares, why the Fe/O type ratios weakly tend to decrease with increasing background SEP intensities. Therefore, the authors of study [127] prefer an alternative interpretation [126]: they consider a large Fe/O ratio to be a manifestation of shock acceleration (Fig. 11) which is effected by quasiperpendicular shocks near the Sun; therefore, this shock accelerates mainly a 'seed' population of flare particles. Since a higher

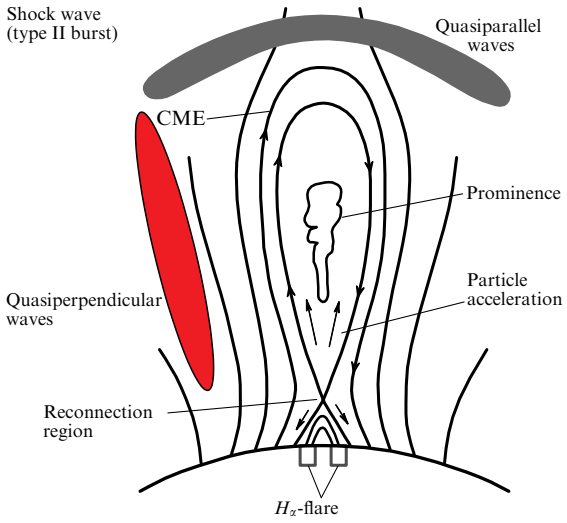

Figure 11. A schematic of possible particle acceleration by quasiparallel and quasiperpendicular shocks generated in a solar atmosphere [26]. In the standard model of eruptive flares, magnetic reconnection in the CME wake gives rise to a two-ribbon flare. If these flare particles escape the CME, they can become seed particles for the subsequent acceleration at the shock wave.

injection energy is needed in the case of quasiperpendicular shocks, these shocks involve a generally smaller seed population in the acceleration process than quasiparallel shocks. As a result, events with quasiperpendicular shocks near the Sun are on the whole characterized by smaller proton fluences, at least at higher energies reached when a shock was close to the Sun.

Turning back to Fig. 11, it should be noted that a large number of schematic pictures of magnetic field topology in the corona in respect to acceleration of solar particles are currently available. These schemes, though merely a convention, can shed light on the cause of different elemental compositions and charge states of accelerated solar ions. Since 1948, the number of such schemes have reached almost 250 (see http://solarmuri.ssl.berkeley.edu/~hhudson/cartoons/)! It should be noted that the scheme presented in Fig. 11 is a result of the long-term evolution of the flare concept [26] greatly influenced by the discovery of CME in 1971, the development of the fundamentals of the shock acceleration theory in the late 1970s, the new paradigm of the predominant role of CME in solar–terrestrial relationships (the early 1990s), and many other cosmophysical factors.

This elegant but rather contradictory picture can be supplemented by the results of Ref. [93] designed to differentiate between restored emission spectra of solar protons, depending on their sources (impulsive or gradual flares and CME-driven shocks). An analysis of several SPEs (including the remarkable GLE42) showed that the recovered number of accelerated particles 'precipitating' in the solar atmosphere and giving rise to outbursts of gamma radiation in lines was systematically smaller than the respective number of runaway particles recorded near Earth as SEPs. This important phenomenon remains unexplored.

The results of an examination of the problem as a whole give strong evidence of the physical link among flares, CMEs, and GLEs. However, its consistent patterns are not strictly determined: in all likelihood, they fit in the 'big flare syndrome' concept proposed 35 years ago [128] and supported by some other researchers (see, for instance, Refs [129, 130]). This view is partly shared by the author of work [127] himself: "In this scenario, the tendency toward a decrease in the abundance ratio with the increasing fluence of soft X-rays and radioemission fluxes at about a 9 GHz frequency can be interpreted in terms of the 'big flare syndrome' [128] which is reduced to the fact that all eruptive event emissions change their scale together: in this case, these events are SEP fluences and peak fluxes of flare electromagnetic emissions."

4.9 Solar flare gamma-rays

High-energy particles accelerated in the solar atmosphere bear the stamp of all properties of the medium in which acceleration occurs and all the processes in which they begin to participate. For example, SCR elemental composition and the energy spectrum reflect the composition of the solar atmosphere and peculiar features of acceleration mechanisms, respectively. Next, accelerated particles lose energy not only in ionizing collisions with atmospheric matter but also to generate a variety of electromagnetic waves, from nuclear gamma radiation to kilometer radio waves. Both the character and the rate of the losses are quite different due to the difference in electron and ion masses. Electrons largely spend energy to ionize the medium and generate bremsstrahlung (X-ray and synchrotron radiation), whereas protons participate in both ionization processes and nuclear interactions in

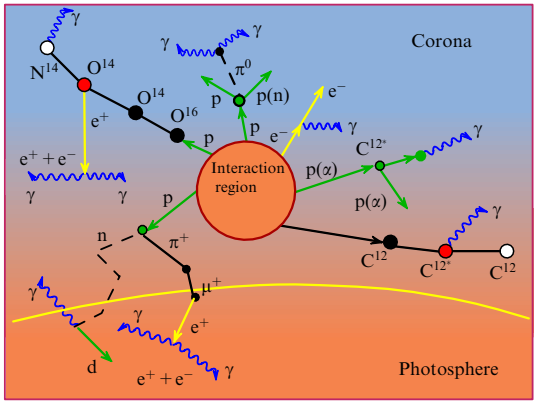

Figure 12. (Color online.) Nuclear reactions in the solar atmosphere induced by SCRs (> 10 MeV/nucleon) (Kotov, 2009). The nuclear reactions are accompanied by the generation of various secondary particles (electrons, positrons, protons, and neutrons), as well as intense gamma radiation (including the 2.223-MeV line from neutron capture by hydrogen nuclei). (Courtesy of Yu D Kotov, MEPhI, Moscow, 2009).

the chromo- and photosphere, where a large number of secondary particles (neutrons, positrons, pions, etc.) are produced and solar gamma radiation is generated (Fig. 12).

Calculations indicate (see, e.g., book [20] and references cited therein for details) that the major contribution to nuclear line generation comes from accelerated protons and alpha-particles with energies of order 1–100 MeV/nucleon. Nuclear interactions of SCRs give rise to secondary neutrons, electrons, and positrons. Annihilation of electrons and positrons in the atmosphere results in production of 0.511-MeV quanta. The capture of neutrons by hydrogen nuclei in the photosphere is accompanied by the emission of gamma quanta with an energy of 2.223 MeV (the so-called neutron capture line). Finally, pions are formed if the energy of an incoming proton exceeds 300 MeV; their decay also produces gamma quanta having a much higher energy (> 90 MeV). Large solar proton fluxes of $\leqslant 100$ GeV are needed to generate flare neutrinos with an energy of $\geqslant 1$ GeV. All these forms of nuclear radiation (including neutrons) are frequently referred to as neutral flare emissions.

Despite a paucity of data on SCR spectra in the sources, they allow the conclusion that accelerated protons, alpha-particles, and other ions have an energy sufficient to excite nuclei of various elements in the solar atmosphere, in the first place C, N, O, and Fe nuclei (Fig. 12). Deexcitation occurs by means of emission of energetic gamma quanta. Radiation is observed in the form of narrow lines characteristic of given nuclei, with some individual ones being capable of emitting a few lines at a time.

The number of lines emitted by nuclei and their intensity are functions of nuclear charge, the type of incoming particle, and its energy. For example, a carbon nucleus emits a most intense 4.444-MeV line upon collision with an accelerated alpha-particle. One of the nitrogen nucleus lines with an energy of 5.105 MeV (not the most intense) arises from its collision with an accelerated proton. An intense 6.129-MeV line of an oxygen nucleus is excited with an equal probability in its collision with fast alpha-particles and protons, etc. An excited iron nucleus also emits a few gamma-lines, of which those with energies of 0.847, 1.238, and 1.811 MeV are of special interest.

4.10 Solar neutrons

Neutral radiation of solar flares including neutrons had been predicted well before it was observed [8]. Flare neutrons were detected for the first time by the SMM satellite on 21 June 1980. On rare occasions, high-energy solar neutrons (up to 400 MeV) can be recorded on Earth's surface by the worldwide network of standard neutron monitors. In the late 1990s, it was supplemented by the worldwide network of five SNTs. The overall neutron event statistics do not exceed 30 cases registered in about 30 years. One of the most notable events occurred on 7 September 2005, when neutron detectors happened to be in the most favorable position (the subsolar point in the Western Hemisphere, afternoon) (Fig. 13).

During the large flare of 4 June 1991, nonstandard detectors recorded events suggesting the birth of solar neutrons with an energy of $\geqslant 10$ GeV [131], corresponding to the energy of accelerated protons of at least $E_p \geqslant 10$ GeV. Clearly, ground-based observations of solar neutrons can be a valuable source of information about acceleration of charged particles at the Sun up to very high energies. Ground enhancements of cosmic ray intensity associated with the arrival of direct solar neutrons are single events in every solar cycle, which accounts for the importance of searching for and interpreting them. They are most probably detected by high-altitude neutron monitors located at sites characterized by high geomagnetic cut-off rigidity (i.e., at the lowest GCR background) in the afternoon hours (local time) at the minimal thickness of the atmosphere. One of the advantages of ground-level recording of flare neutrons is that solar neutrons are not vulnerable to variations under interplanetary conditions even if their flux is most intense only at a subsolar point on Earth's surface. Moreover, some of them disintegrate as they travel toward Earth and fail to reach it. Nevertheless, the most energetic of them (tens and hundreds of MeV) can be recorded by ground-based NMs and the SNT network.

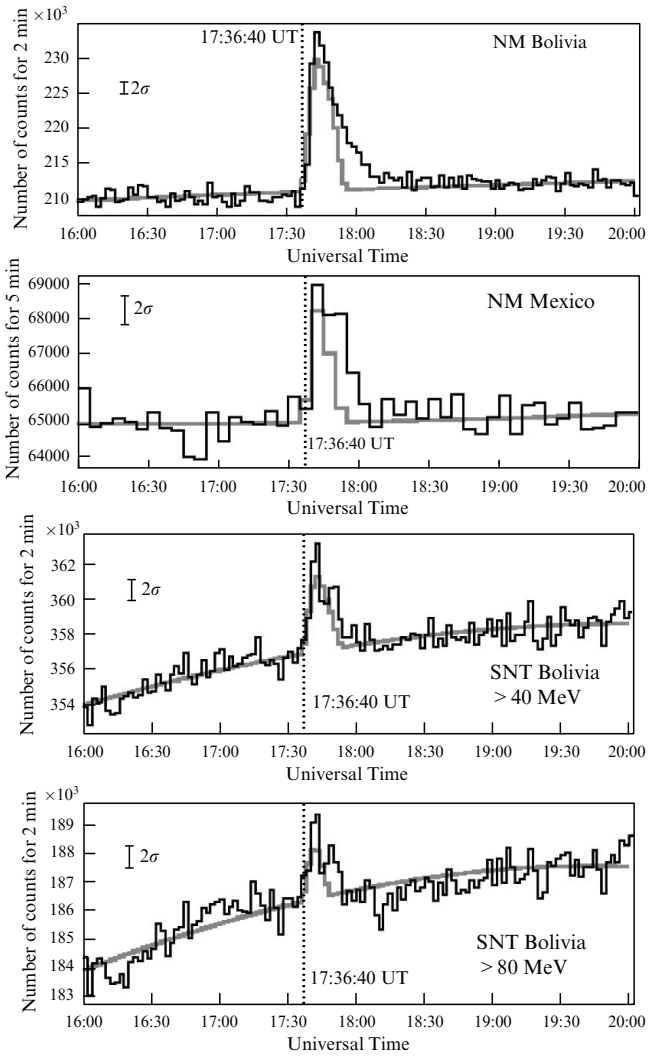

Figure 13. Registration of solar neutrons associated with the flare of 7 September 2005 [134]. From top to bottom: data obtained with 2 min intervals using the NM located at Mt. Chacaltaya (Bolivia), with 5 min intervals using the NM station in Mexico, and with 2 min intervals using the channels with threshold neutron energies of > 40 and > 80 MeV of the SNT in Bolivia.

Solar flare neutrons have been detected many times by the worldwide network of neutron monitors (see, for instance, monograph [20] and references cited therein). An interesting neutron event was reported, in particular, from the neutron monitor located at the Mount Norikura station in Japan on 4 June 1991 [132] after the strong X12.0/3B flare (N30°, E70°). Characteristically, the counting rate profile of the Norikura NM exhibited two maxima, at 03:41–04:10 and 04:15–05:05 UT. Despite the rather small time interval between the two peaks, detailed analysis of the event with the use of intensity–time profiles of 2.223-MeV gamma radiation (CGRO/OSSE orbital laboratory) and microwave radiation (Nobeyama Observatory) enabled the authors of report [133] to conclude that neutron generation can be a time-consuming process. At any rate, the second episode of particle acceleration in the Sun was documented roughly 30 minutes after the impulsive phase of the flare. At this moment, the CME front was far from the Sun, and protons accelerated at a shock wave could not generate the observed neutrons. This event was not included in the statistics of 72 GLEs, but a minor SPE of maximal intensity (~ 325 pfu) in the energy region of > 10 MeV was recorded in Earth's orbit [59].

There are reports on recording solar neutrons during GLE69 of 20 January 2005 [133]. However, the most interesting neutron event is that of 7 September 2005 [134], measured with a high statistical accuracy (Fig. 13) in association with the giant 3B/X17 flare (S06°, E89°).

The strongest soft X-ray blast was registered by the GOES-11 spacecraft at 17:40 UT, and the initiation of type II radio burst at 17:42 UT. According to the detector aboard the GEOTAIL satellite, the outburst of hard X-ray radiation (> 50 keV) reached a maximum at 17:36:40 UT, while the INTEGRAL space laboratory recorded 1-MeV gamma radiation. Because the nuclear lines were indistinct, the observed gamma radiation was ascribed to accelerated high-energy electrons. The most favorable conditions for observations with neutron monitors and solar neutron telescopes took place in Latin America.

Figure 13 demonstrates the results of observations in Mexico and Bolivia. To begin with, it shows neutron peaks recorded with 5-min and 2-min intervals by neutron monitors located in Mexico City (Mexico) and at Mt. Chacaltaya (Bolivia), respectively. Also shown are data obtained with 2-min intervals using two energy channels of the solar neutron telescope in Bolivia with threshold neutron energies of > 40 and > 80 MeV. The instant of 17:36:40 UT corresponds to the time maximum for the flux of a hard X-ray emission measured aboard the GEOTAIL spacecraft. Grey curves

show expected (calculated) neutron counting rates based on the results obtained with the use of the Bolivian NT.

Importantly, an eastward CME was documented at 17:23 UT on 7 September 2005. It appears that the eastern-most location of the flare prevented protons with a relativistic energy from reaching Earth's immediate environment and ground-based stations from recording a 'classical' GLE. Nevertheless, the NOAA Space Environment Center (SEC NOAA) (http://www.sec.noaa.gov/) reported the beginning of a strong CME in Earth's orbit at about 02:15 UT on 8 September with a proton flux of > 10 MeV that reached a maximum of 1880 pfu at 04:25 UT on 11 September.

5. Long-term variations

This section is focused on some peculiar features of SPEs characterizing the behavior of SCR fluxes and fluences of different energies on a long-term scale with special reference to the following issues: (1) annual variations in the number of SPEs for $\geqslant 10$ MeV protons in 1955–2015, (2) time distribution of SCR events with energies of $\geqslant 10$, $\geqslant 100$, and $\geqslant 433$ MeV over the entire observation period, and (3) the dynamics of GLE recording rate during the period from 1942 to 2015.

5.1 Annual variations in the number of SPEs

Figure 14 illustrates the behavior of annual average numbers of SPEs, N_y, for $\geqslant 10$ MeV protons in comparison with the solar activity index (the number of sunspots W_y). N_y values presented in Ref. [135] were estimated largely from a few SPE catalogs [54–60]. The data on proton events meeting the SEC NOAA ($\geqslant 10$ pfu) criterion were used for the period of 2010–1015 (solar cycle 24) [61]. Solar activity indices W_y are presented on two scales; the traditional one (Wolf number), and the recently proposed new scale (http://sidc.oma.be).

Notwithstanding a number of methodical difficulties encountered in the choice of events that had taken place before the 'space era' (1955–1965), certain behavioral features of the annual average number of SPEs are exhibited fairly well. Specifically, the so-called 'Gnevyshev Gap' is quite apparent, i.e., the temporary depression ('valley') close to the solar activity maximum in the double-peaked structure of the N_y – time profile. This effect was named after the Soviet astronomer M N Gnevyshev, who initiated investigations into the doubled-peaked structure of SA cycles [136]. The above data are of great interest for surveying the general solar proton emissivity and long-term trends in the behavior of the solar magnetic fields. Moreover, the data in Fig. 14 may be useful for the development of methods for the long-range prognosis of radiation conditions in outer space (see, e.g., review [137]).

5.2 Time distribution of SCR events

The data of SPE catalogs can be used to describe the behavior of SPE amplitude, depending on SA index for solar particles of various energies. Figure 15 illustrates the time distribution of SCR events at a proton energy of $\geqslant 10$ MeV, $\geqslant 100$ MeV, and $\geqslant 433$ MeV (GLE) during the respective observation periods [138]. For $\geqslant 10$-MeV and $\geqslant 100$-MeV protons, the absolute values of maximum fluxes are presented in pfu; the values for GLEs are given in percent of the pre-flare GCR intensity.

Figure 15 illustrates both the history of SCR research (e.g., omissions of weak GLEs at the earlier stages of their examination) and peculiarities of the SPE/GLE occurrence rate, depending on the SA index and progress in the development of measuring techniques. Highly noteworthy is the Sun's 'weakness' in the 24th activity cycle in terms of the sunspot number, the number of 'usual' SPEs (see also Fig. 14), and especially the number of GLEs.

5.3 Rate of GLE registrations

Another interesting aspect, which characterizes the Sun as a star, was revealed as a result of a wavelet analysis of the GLE occurrence rate η depending on the SA level (sunspot number) and solar cycle epoch [139]. Using the dates of events from

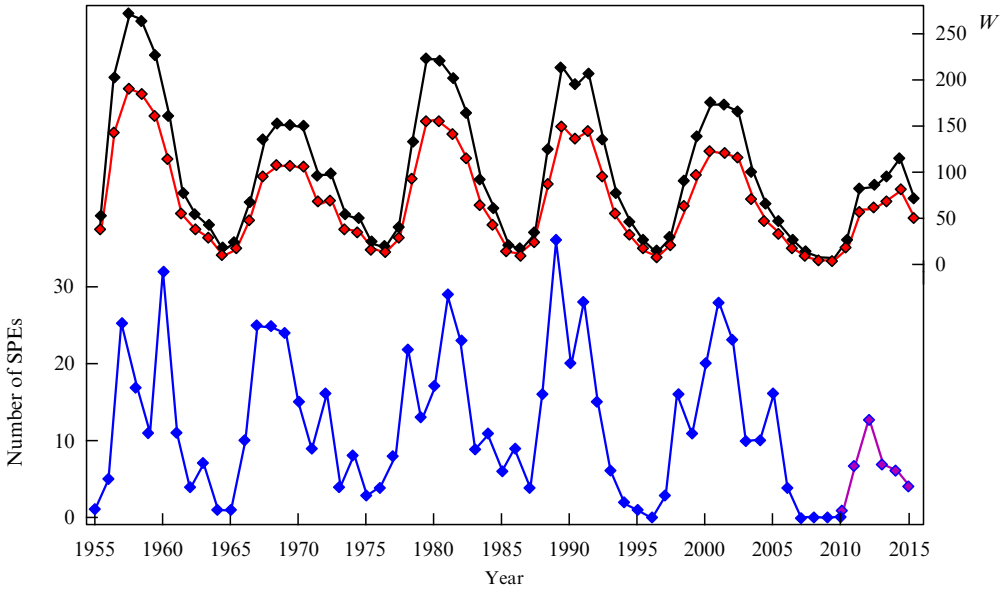

Figure 14. (Color online.) Annual average number of SPEs, N_y, [135] for protons with an energy of > 10 MeV and maximum intensity > 1 pfu (lower blue curve) in comparison with the SA index during the period from 1955 to 2015 (two upper curves). The SA index is presented on two scales: old (Wolf number W_y) and new (sidc.oma.be) by red and black symbols, respectively. The number of SPEs in the 24th solar cycle (violet symbols) is estimated based on the NOAA SEC criterion (www.swpc.noaa.gov/ftpdir/indices/SPE.txt).

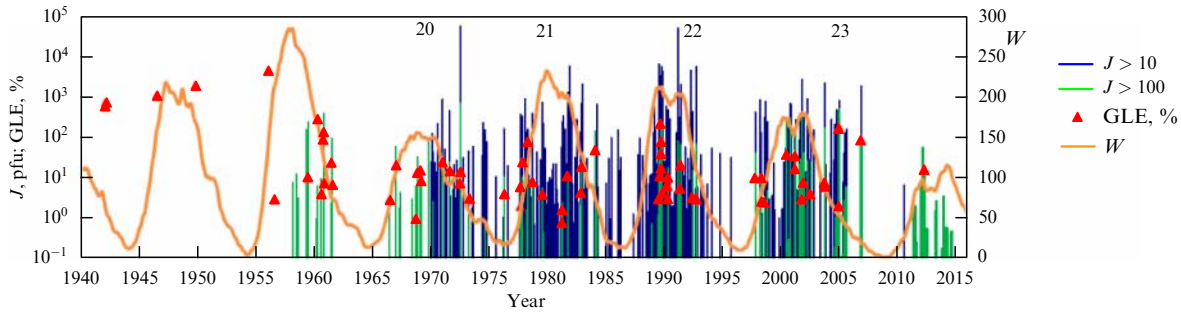

Figure 15. (Color online.) Time distribution of SCR events with various energies (Bazilevskaya: 2016, All-Russian Cosmic Ray Conference, Dubna, August 2016). Adapted from Ref. [138].

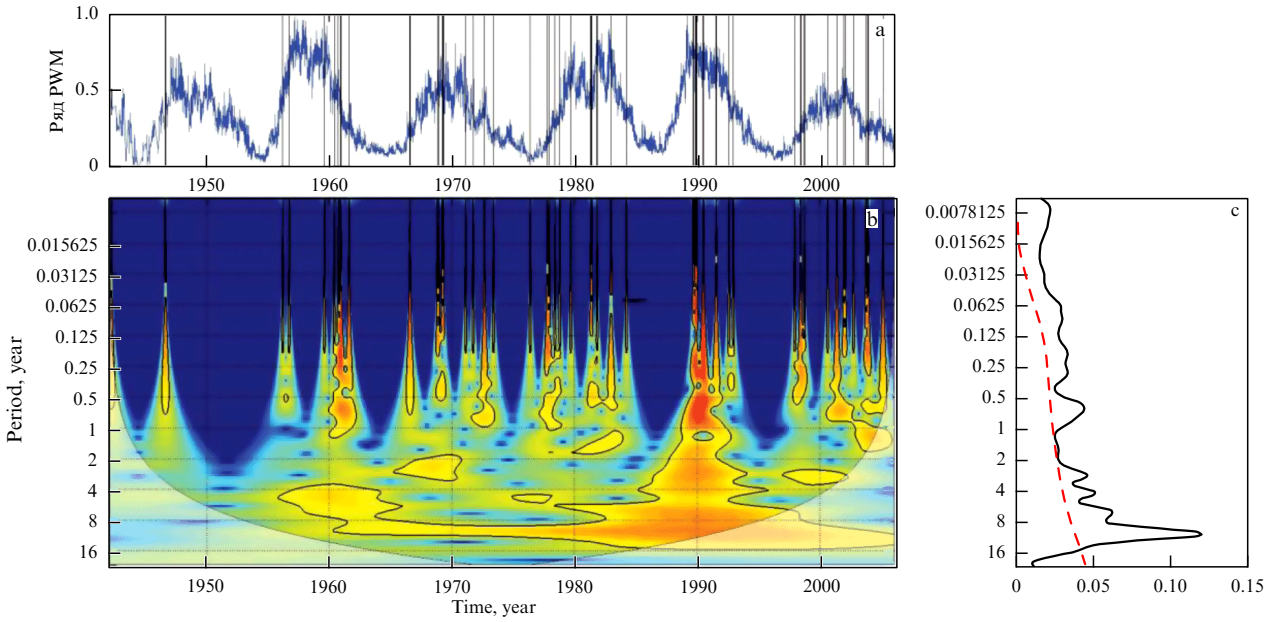

Figure 16. (Color online.) Oscillations of the GLE registration rate [139]. (a) PWM time series for the registration rate was constructed by the Morlet method using the dates of 70 events between 1942 and 2006. (b) Wavelet-diagram for the oscillation spectrum (periods are indicated on the left in fractions of the year along the axis of ordinates). (c) The oscillation power density spectrum in arbitrary units (x-axis) depending on the period (in fractions of the year) (y-axis). The dashed line corresponds to the red noise level.

Table 1 [15] and the Morlet method (pulse width modulation, PWM), we constructed a PWM series for parameter η which includes the statistically significant oscillation with a period of $\sim$ 11 years (Fig. 16), the amplitudes of remaining oscillations being comparable to the noise level. In this case, η oscillations are to a certain degree coherent with the time series of the parameters of the photosphere (sunspot number S) and corona (coronal index – CI). Solar flares being the main source of large GLEs, a similar coherence should be expected when using the solar flare index (SFI) that serves, together with the coronal index, as an indirect (proxy) characteristic of the SA level [140]. In spite of the limited GLE statistics and limits of applicability of the wavelet analysis method, these results can be interesting for understanding GSMF behavior and quasiperiodic phenomena in the solar dynamo, the solar atmosphere, the interplanetary medium, and cosmic rays.

As was established earlier, GLEs tend to group mainly on the ascending and descending branches of solar cycles (see Figs 15 and 16a) apparently due to the specific features of the spatio–temporal structure of the global solar magnetic field (GSMF). As is known, this field reverses its sign precisely near SA maxima. In this context, the results of Ref. [141] are worth mentioning. The authors of paper [141] used MT and NM data for 43 GLEs detected between 1942 and 1990 to analyze the above GLE tendency. They showed that the flares responsible for initiation of GLEs are basically forbidden during the cycle transient phase, when the GSMF reverses its sign. The absence of GLEs in an SA maximum is explained by impaired efficiency of particle acceleration during the GSMF reconfiguration rather than by suppression of SCR escaping under the effect of strong magnetic fields.

Because certain periodicities found in Ref. [139] are coherent for parameters η, S, and CI, it can be concluded at this stage of the study that oscillations are synchronized in different layers of the solar atmosphere: from the photosphere to the corona. This can indicate that SCR generation (GLE) is not a local (isolated) process but involves wide areas in the solar atmosphere.

6. Event distribution functions

GLE distribution over absolute intensity is of great interest in the context of evaluation of the maximum potential of a solar accelerator (accelerators). Equally interesting is the problem

of proton emissivity of the Sun in comparison with that of other stars. In a broader, astrophysical context, the problem reduces to a comparison of the energetics of solar and other stellar flares.

6.1 GLE distribution

The authors of Ref. [135] have recently attempted to construct an integral GLE distribution from absolute proton fluxes with rigidity $R > 1$ GV, based on the set of I_{max} estimates (> 1 GV) in pfu for 71 events available from the literature. They also re-estimated certain values [135]. The distribution function thus obtained is presented in Fig. 17.

To recall, the values of $I_{max}(> 1$ GV) are accurate up to a factor of ~ 2.0. One of the noticeable results of Ref. [135] is that most values of $I_{max}(> 1$ GV) for SCRs proved higher than the integral intensity of GCRs at equal rigidity, i.e., $I_{GCR}(> 1$ GV) $\geqslant 1$ pfu, as reported earlier in Ref. [142].

On the other hand, Fig. 17 demonstrates an almost flat integral GLE distribution in the low-intensity region. This once again emphasizes the importance of small-amplitude GLE ('hidden GLE') studies for better understanding the SCR spectrum formation, especially in the relativistic energy region (see, e.g., paper [63]).

6.2 Flares on the Sun-like stars

Very interesting aspects of the SCR problem have emerged quite recently in connection with new observations of superflares on other G type Sun-like stars [143, 144]. As is well known, the absolute magnitude of Sun's luminosity is +4.83. The Sun is assigned to the G2V spectral class comprising stars that exhibit strong metal absorption lines in their spectra. Class 2G encompasses stars having a temperature of ≈ 5800 K (yellow dwarfs) at the surface (photosphere). Sun-like stars are slowly rotating bodies with surface temperatures close to that of the Sun (5600–6000 K) and a period of rotation of more than 10 days.

The authors of Ref. [143] have recently identified 365 superflares on Sun-like stars, based on the events registered by the Kepler spacecraft. These observations give evidence that superflares are associated with much greater spots than sunspots and occur much more frequently on rapidly rotating stars. The authors of Ref. [143] distinguished among the 365 flares 14 superflares that occurred on Sun-like stars (slowly rotating main-sequence G type stars having a rotation period of more than 10 Earth's days and the effective surface temperature within 5600 K $< T_{eff} <$ 6000 K). These data were used to estimate the rate of superflares with different

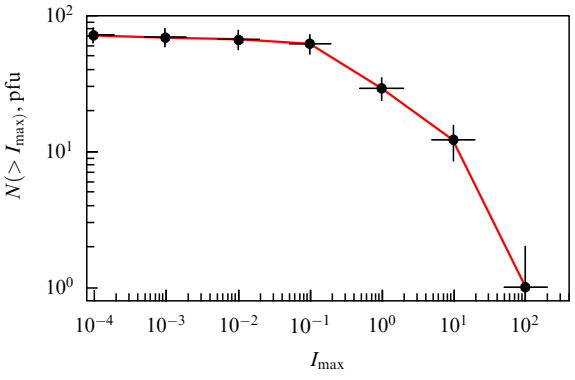

Figure 17. Integral distribution of 71 GLEs in 1942–2014 in terms of SCR fluxes (in pfu) at particle rigidity $R > 1$ GV [135].

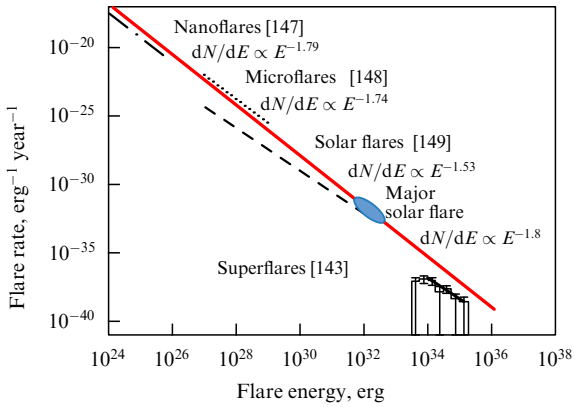

Figure 18. (Color online.) Superflare rate on G type stars (histogram at bottom) [144] in comparison with the rate of solar flares. Solid thick line in the histogram shows the differential distribution of superflare rate on Sun-like stars with exponent equal to 1.5 ± 0.3. Dashed, dotted, and dashed-dotted lines show power-like distributions of solar flares in the extreme UV region [147] and in soft [148] and hard [149] X-ray regions, respectively. The thick red line corresponds to the theoretically expected power-like function with increment 1.8 [147]. The blue oval is the most powerful solar flare.

energies. It was found that one flare is likely to occur on the Sun once every 800 years at an energy of $\sim 10^{34}$ erg, and once in 5000 years at an energy of $\sim 10^{35}$ erg. Simple calculations in Ref. [144] in combination with analytical results [143] showed that, at the present-day level of solar activity, superflares with an energy of $\sim 10^{34}$ erg can occur once every 800 years. To recall, the energy of the solar flares documented thus far was 1% of that.

In addition to these estimates, it should be noted that the differential distribution of superflares over energies has a power-like shape with exponent $\alpha_G = 1.5 \pm 0.3$ [144] close to the exponent $\alpha_S = 1.8$ of sunspot distribution (Fig. 18). Moreover, it was shown in Ref. [145] that the exponent $\alpha_X = 1.98 \pm 0.11$ for peak fluxes of soft X-ray radiation remains unaltered (invariant) during three solar cycles. Actually, only this type of solar (flare) activity has a conclusive theoretical explanation: the value of α_X agrees with the predicted $\alpha_F = 2.0$ value ensuing from the model of fractal-diffusive self-organized criticality (FD-SOC) for solar plasma [146].

Interestingly, superflares on Sun-like stars, as well as solar flares, microflares, and nanoflares, are arrayed approximately along a single line corresponding to the power law with exponent 1.8 (solid red line in Fig. 18) for a broad region of energies from 10^{24} to 10^{35}erg.

7. Extreme ('ancient') SCR events

The field of research on SCR events that occurred before the advent of instrumental observations is sometimes referred to as cosmic ray archeology. This term was introduced by Shea and Smart [150] with a view to using indirect data (*proxy data*) on possible witnesses of the past instead of direct measurements. In other words, it was proposed to learn to extract information from natural 'archives' where past events were imprinted and are believed to be stored in the original form [19]. The first candidates for the role of such witnesses are cosmogenic isotopes (radionuclides), including radiocarbon ^{14}C, as well as ^{10}Be, ^{36}Cl, ^{26}Al, etc., formed under the effect of cosmic rays in lunar and planetary matter, meteorites and cosmic dust, the oceans, and Earth's surface and atmosphere.

Solar cosmic rays also make a contribution to radionuclide synthesis.

At present, the most detailed data on cosmic ray variations in the past are obtained from studies of the radiocarbon (^{14}C) content in organic remnants, e.g., tree rings and humus (radiocarbon analysis), as well as beryllium isotope ^{10}Be in polar ice and bottom sediments in lakes or oceans. This technique has found wide application in various scientific disciplines, from archeology to cosmic physics, since the late 1940s. An instructive example is provided by Refs [151, 152] describing a rise in ^{14}C content in tree rings documented in 1943 and making a conclusion about the possible relation of this effect to the first GLEs of 28 February and 7 March 1948 (see Fig. 2).

Other important 'witnesses' of past events in the Sun–Earth system are nitric oxides (NO_x) or, rather, some end products (nitrates) of the nitrogen cycle in the atmosphere, including binary compounds of nitrogen and oxygen from NO to N_2O_5, as well as mixtures containing several like constituent components. Nitrogen oxides are formed in Earth's atmosphere under the effect of cosmic rays (SCRs and GCRs) and fall to Earth's surface as precipitation (rain and snow), where they become literally frozen in Greenland and Antarctic ice. Ice core samples contain 'nitrate signals', i.e., an elevated NO_x concentration, giving strong evidence of the intrusion of additional cosmic ray fluxes into Earth's atmosphere. The use of this technique has allowed effects of individual large solar flares to be revealed and analyzed [153–155]). Today, they are known as 'extreme' proton events.

7.1 Concept of extreme SCR events

The notion of 'extreme SCR events' in solar cosmic rays is the subject of divergent interpretations [20]. Some regard an event as extreme if the worldwide network of CR stations record the arrival of an appreciable flux of relativistic solar protons (GLEs) at Earth. Alternatively, an extreme event is defined as a large SCR flux registered in Earth's orbit, mostly in the nonrelativistic region. To recall, the SCR spectrum spans a few orders of magnitude of the flux on the energy scale, with relativistic particles making up only part of it. Therefore, the use of the acronym SEPs along with SCRs seems fully justified, and the term SEP event (or SPE) has an even more general meaning for the description of accelerated particles of a solar origin.

On the other hand, $\sim$ 10–100-MeV solar protons are usually considered to be 'most efficient' when it comes to the evaluation of radiation hazard on circumterrestrial and interplanetary routes. The typical effective energy is 30 MeV (for protons). In dose calculations, the integral $\Phi(\geqslant 30$ MeV) fluence in protons/cm^2 rather than SEP flux energy is used. Therefore, only an event in which $\Phi(\geqslant 30$ MeV) is higher than a certain chosen value can be defined as extreme. In other words, extreme events are definitely powerful SPEs. In this context, an event with the *largest* $\Phi(\geqslant 30$ MeV) fluence chosen from all the observed events can be regarded as extreme. In practical terms, such an event is an example of the 'worst case' when it comes to the evaluation of radiation hazard in outer space and the calculation of selected geophysical effects driven by solar cosmic rays.

Up to the present time, the 'worst case' has been exemplified by the so-called Carrington event (CE), recorded on 1–2 September 1989. Observation of this event gave an impetus to instrumental studies in solar flare physics, while subsequent geophysical perturbations (auroras, strong magnetic storm, etc.) confirmed its extreme character. The integral CE fluence of $\Phi(\geqslant 30\ \text{MeV}) = 1.88 \times 10^{10}$ cm^{-2} exceeded fluences of all the events detected by the nitrate method [155] from the content of nitrogen oxides in the Greenland ice core for the period from 1561 to 1950. Therefore, this CE was designated as the 'worst case' in the sense of the above definition [156, 157]. Indeed, the two most probable candidates for this role, viz. the events of 15 November1960 and 4 August 1972, were characterized by much smaller $\Phi(\geqslant 30\ \text{MeV})$ fluences (around 9×10^9 cm^{-2} and 5×10^9 cm^{-2}, respectively) [158].

7.2 Biggest SCR events in the past

One of our previous studies [157] was highly motivated by the publication of new data on proton fluences for a number of large events during the period between 1561 and 1994, part of which was identified by the nitrate method [155]. The complete list presented in Ref. [155] contains 12 major events with the $\Phi(\geqslant 30\ \text{MeV}) \geqslant 6 \times 10^9$ cm^{-2} fluence. All the estimates were obtained using Greenland ice core samples: 7.1×10^9 (1605); 8.0×10^9 (1619); 6.1×10^9 (1637); 7.4×10^9 (1719); 6.3×10^9 (1727); 6.4×10^9 (1813); 9.3×10^9 (1851); 1.88×10^{10} (1859, CE); 7.0×10^9 (1864); 7.7×10^9 (1894); 1.11×10^{10} (1895); 8.0×10^9 (1896).

These data were analyzed and interpreted in Refs [156, 158]. Some later researchers questioned the validity of the 'nitrate signal' itself for the Carrington event [159, 160] and, accordingly, the reliability of the findings reported in Ref. [155]. We think that these doubts are not altogether baseless, but they do not compromise the possibility of using CE along with other events included on the list in Ref. [155] for updating the SPE distribution function in terms of $\Phi(\geqslant 30$ MeV) fluences (see Section 7.3). Such an approach may help also resolve doubts [159, 160].

About 10 years after the appearance of the fundamental study [155], the authors of Ref. [161] published a new list of 23 large 'ancient' SPEs with fluences of $\Phi(\geqslant 30\ \text{MeV}) \geqslant 10^{10}$ cm^{-2} that are likely to have occurred in the past on the $\sim$ 100–1000 year time scale. The $\Phi(\geqslant 30$ MeV) values were estimated from 'archaeological data' on cosmogenic isotopes ^{14}C and ^{10}Be, assuming that candidate events developed in accordance with the so-called GLE05 scenario, i.e., the scenario of the known event of 23 February 1956 that is thus far considered to be the *biggest* one in terms of particle flux and fluence in the *relativistic* energy region. Notice, however, that the GLE05 scenario is vulnerable to criticism, first of all on the grounds that the spectrum of nonrelativistic protons on 23 February 1956 was rather smooth (see, for instance, Ref. [17]), and the $\Phi(\geqslant 30$ MeV) fluence did not exceed $\sim 10^9$ cm^{-2} [150]. At the same time, all the events listed in Ref. [161] deserve the most thorough further examination.

A few years ago, radiocarbon analysis revealed a ^{14}C spike around 774–775 AD (hereinafter referred to as AD775) based on measurements in old tree rings in Japan, Europe, Russia, and America by virtually independent research groups [162–164]. At present, the highest $\Phi(\geqslant 30$ MeV) fluences calculated from these data amount from $(2.07-2.96) \times 10^{10}$ cm^{-2} [157] to 4.5×10^{10} cm^{-2} [163] and 8.0×10^{10} cm^{-2} [167]. Some way or another, the AD755 event can now be believed as a most likely candidate for the role of the 'worst case'. Notwithstanding some doubts and controversies as regards the reliability of $\Phi(\geqslant 30$ MeV) estimates and even the nature (source) of AD775 event ([157, 165–168]), we use in Section 7.3

all the available data to construct the new SPE distribution function in terms of integral $\Phi(\geqslant 30$ MMeV) fluences [157] within the maximum range of the currently accessible fluence values.

7.3 New distribution function

To approximate the fluence data, we took advantage of the following function (Fig. 19):

$$\Psi(\geqslant \Phi) = \left(\frac{\Phi}{10^6}\right)^{-\gamma}\left(\exp\frac{\Phi}{\Phi_0}\right)^{-1}, \qquad (7)$$

where γ is the exponent, $\Phi \equiv \Phi(\geqslant 30$ MeV), and Φ_0 is the characteristic constant of the exponential factor. Such a form for the distribution function appears to be universal for any manifestations of solar flares, e.g., peak fluxes or fluences in outbursts of X-ray and radio emission, proton and electron emission, etc. The solid line in Fig. 19 corresponds to formula (7), the vertical bars indicate error margins (root-mean-square deviations), and the blue rectangle characterizes the uncertainty of AD775 fluence estimations. An approximation of the fluence distribution function using relation (7) seems reasonable at the following parameters: $\gamma = 0.32$, and $\Phi_0 = 7 \times 10^9$ cm^{-2}.

To sum up, the appearance and investigation of crucially new archive data on 'ancient' proton events greatly promote further advancement of such practically important issues as the evaluation of the probability of the arrival of 'extreme' SCR fluxes at Earth (at least such as are conceivable based on the mean SA level in the modern epoch). A combination of model (7) and the SCR upper limit spectrum (ULS, see Section 3.4) model opens up the possibility for a new approach to the 'worst case' concept with reference to the Carrington and AD775 events, providing the key points for normalization. Such prospects look very promising for simulating and calculating radiation doses.

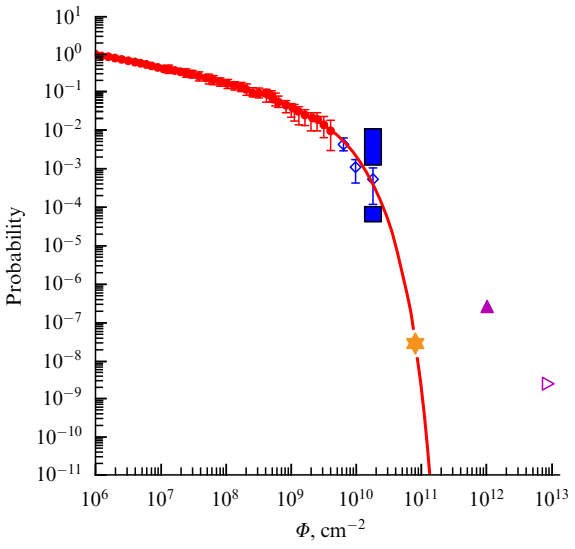

Figure 19. (Color online.) SPE distribution function over integral proton fluences $\Phi \equiv \Phi(\geqslant 30$ MeV) taking account of the last data on 'ancient' extreme events. Red dots — data of direct satellite measurements ('cosmic era'); blue diamonds — estimates obtained by the nitrate method [155], including the Carrington event. Blue rectangle denotes AD775 event with due regard for the last estimates (see Addendum). Violet triangles on the right (dark and light) — integral fluences $\Phi(\geqslant 30$ MeV) for extrapolation into the past (1 mln and 100 mln years, respectively) [157] based on the data from [169]. Orange asterisk — maximum fluence $\Phi(\geqslant 30$ MeV) estimated from cosmogenic isotope content in lunar bedrock (see Addendum).

8. Geophysical and applied aspects

Due to the strong ionizing action, SEPs (solar particles having energies on the order of tens and hundreds of MeV) play an important role in many geophysical processes [17, 19, 20, 138, 170]. Their well-known effects include ozone layer depletion, perturbations in the global atmospheric electrical circuit, and generation of nitrates and cosmogenic isotopes, not to mention other phenomena still poorly explored or anticipated (but unproven). We shall consider in brief the contribution of relativistic solar protons to these effects. It is worthwhile to note that energy density and total energy brought by SCRs into Earth's atmosphere are incomparable to the energy coming to the circumterrestrial space from other sources. For this reason, SCRs cannot be the main cause of geophysical perturbations (e.g., in comparison with CME or geomagnetic storms). However, the arrival of SEPs can be an important (triggering) component of the global mechanism underlying solar–terrestrial relationships. In Sections 8.1 and 8.2, we will present only two characteristic examples of SCR effects in Earth's atmosphere and briefly discuss attempts to use results of ground-based observations for the prognostication of SCR fluxes falling on Earth.

8.1 Atmospheric SCR effects during GLE

SEP penetration into the polar atmosphere inevitably modifies the composition and physical–chemical processes in both the mesosphere and stratosphere [171, 172]. The authors of report [171] evaluated the influence of SEPs on these processes during three GLEs recorded in October 1989, July 2000, and April 2001 in a wide energy range, with due regard for the evolution of their spectra. Much attention was given to generating nitrogen oxides NO_x and hydroxides HO_x, as well as to changes in the ozone O_3 content. The results of calculations for different events were compared among themselves. The analysis was performed with the use of a model taking into account particle penetration into and deposition in the atmosphere, as well as the resulting modification of atmospheric chemistry.

In October 1989 (Fig. 20), a high level of ionization was first documented in the lower stratosphere, while that in the

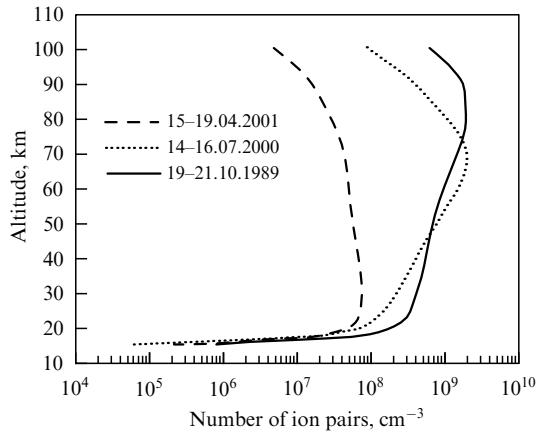

Figure 20. Comparison of altitudinal ionization profiles in Earth's atmosphere during three GLEs, taking into consideration the contribution from solar protons with energies up to 500 MeV [171].

mesosphere was an order of magnitude smaller. Thereafter, ionization in the lower stratosphere remained unaltered (due to the almost constant intensity of high-energy particles), whereas mesospheric ionization significantly increased as a consequence of the arrival of low-energy particles whose intensity continued to grow. Ionization variation patterns in July 2000 were more complicated than in October 1989: enhanced ionization of the middle mesosphere was concurrent with its reduced level in the upper mesosphere. Because the intensity of high-energy particles began to decrease early enough, the ionization rate in the stratosphere declined, too, as the event continued to evolve. The ionization rate increased with time only in the upper mesosphere. The calculated ionization profiles for the event of April 2001 were comparable to those for the event of October 1989, even if the absolute ionization rates were lower by a factor of 2 or 3. Nevertheless, ionization level decreased with time at all altitudes. The model yielded similar results when extrapolating proton spectra to 500 and even 800 MeV.

Analogous studies of GLE70 (13 December 2006) were reported in Ref. [172]. The authors evaluated the effect of SEPs on the chemical composition of the middle atmosphere (20–80 km). Proton spectra were deduced from NM data, measurements in the stratosphere, and spacecrafts. The generation and loss of minor atmospheric constituents during GLEs were calculated using a one-dimensional model developed by the authors in an earlier study, taking into consideration its time dependence. The estimates of the ozone layer depletion rate proved consistent with the data of the Microwave Limb Sounder (MLS) aboard the AURA spacecraft. The authors concluded that the main factor responsible for the reduced ozone content in the middle atmosphere during precipitation of solar protons was the generation of odd HO_x constituents followed by recombination of ionization products.

8.2 Generation of cosmogenic isotopes

This section is devoted to the known effect of the generation of cosmogenic isotopes by cosmic rays in Earth's atmosphere as exemplified by a recent paper [173]. The authors undertook new detailed calculations of the generation rate (power) of cosmogenic isotopes ^{3}H, ^{7}Be, ^{10}Be, and ^{36}Cl applying the FLUKA (Monte Carlo code) simulation package and taking account of the recent data on interaction cross sections of vertically incident protons with energies from 10 MeV to 10 GeV. This made possible an investigation of the isotope generation by both SCRs and GCRs in the low-energy region where generation power is a highly sensitive function of energy. It was shown that the ^{10}Be generation rate in the events of October–November 2003 reached a maximum at ~ 100 MeV, whereas ^{7}Be and ^{36}C1 were most efficiently produced at an energy of ~ 25 MeV with the 'resonant' cross section of the process. In the case of a steeper SCR spectrum than the one observed in October–November 2003, the maximum of generation power is displaced toward lower energies, whereas the peak for the more flat spectrum (20 January 2005) shifts to the high-energy region. The total integral generation of ^{7}Be and ^{36}Cl by SCRs in the 2003 events is three times that of ^{10}Be due to the 'resonance' effect manifested at the energy of ~ 25 MeV of protons that generate isotopes ^{7}Be and ^{36}Cl by nuclear disintegration of atmospheric nitrogen ^{14}N and argon ^{40}Ar, respectively.

An analysis of annual generation of ^{10}Be shows that only the extreme event of 23 February 1956 could make an important contribution to the production of this isotope. Annual generation of ^{36}Cl was roughly 2–5 times higher, depending on the SCR spectrum shape. The authors of Ref. [173] calculated the annual generation of ^{10}Be, ^{36}Cl, and other isotopes at the geomagnetic latitude $> 65^{\circ}$ in the period from 1940 to 2006, during which six 11-year solar cycles took place. The mean amplitude of the 11-year variation in annual content of these isotopes proved to be around 1.77. With due allowance being made for the latitudinal mixing, the amplitude decreased to 1.48 for mean global generation.

8.3 SCR in prognostic schemes

The application of numerous methods and schemes for heliogeophysical predictions in the mid-1980s brought researchers to the idea to use ground-based observations of cosmic rays for short-term forecasting of various phenomena. Specifically, it was proposed to employ relativistic solar protons with $R \geqslant 1$ GV as a predictor of SPEs in the nonrelativistic region. The authors of Ref. [174] were the first to consider the possibility for diagnostics of the interplanetary medium and the prediction of the onset of SPEs based on the solution of the reverse problem of SCR transport. They intended to use GLE observations up to the SCR maximum in Earth's orbit to reconstruct their emission function in the Sun and thereafter predict the development of SCRs for some hours to come.

Although the methodical aspects of such an approach were fairly well substantiated, it remained unclear how to verify the proposed scheme based on observational data. A difficulty was posed by the fact that a large flux of relativistic protons was not invariably accompanied by a similarly enhanced flux in the nonrelativistic region (see Fig. 8); in other words, the problem of the shape of SCR spectrum in the source arose. The role of relativistic SCRs in the prognostic schemes was later considered in many publications [175–180]. For example, the authors of Ref. [175] developed an empirical approach to determining the solar proton spectrum near Earth in an energy range between 10 MeV and 10 GeV directly from observational data without any preliminary tentative assumption as regards its shape. This method also permitted the reconstruction of the intensity–time profile for protons of any energy. An interesting alert algorithm for the arrival of SCRs and automatic determination of their spectrum was developed in Ref. [176] using 1-min NM data from the worldwide network (NMDB).

The authors of Ref. [177] attempted to predict the shape of the spectrum of maximum fluxes of nonrelativistic protons during SPEs from the data on the delayed component spectrum in the respective GLE. They regarded the proton spectrum in the $\leqslant 500$ MeV region as a natural gradual continuation of the delayed component spectrum and demonstrated an excellent agreement between the delayed component spectrum and its extrapolation into the low-energy region ($\leqslant 433$ MeV), in which direct measurements by the Meteor spacecraft and balloon-borne instruments were made in the stratosphere. The authors proposed a reasonably limited model that used data from almost 20 neutron monitors, making it possible to obtain SCR spectra in real time with an accuracy sufficient for short-time prognosis and to address a variety of space weather problems in an automatic mode.

However, further studies revealed that the above schemes are as yet only of a preliminary character and cannot be expected to provide a comprehensive solution to

the problem. The authors of Ref. [178] evaluated results of the application of the method proposed in Ref. [179] for early warning about the arrival of solar protons with $E_p \sim 10-100$ Mev based on the NMDB. The retrospective analysis and comparison with observations of 2001–2006 showed that more than 50% of the solar proton events were missed using this forecast method. To improve its prognostic value, additional data on the Sun's and heliosphere activities are needed.

A new approach to GLE prognostication was proposed in Ref. [180] based on varying the GLE registration rate (see, for instance, Ref. [139] and Fig. 16). The primary objective of this work [180] was to develop a method for the prediction of such events during the 24th cycle of solar activity. A preliminary prognosis predicted the next GLE71 between 12 December 2011 and 2 February 2012. The event actually occurred on 17 May 2012. It was weak and could be observed only at high latitudes (see Fig. 4). Maximum enhancement ($\sim 23\%$ based on 5-min NM data) was recorded at the South Pole. However, further development of this approach [181] using wavelet analysis of the GLE occurrence rate (see Section 5.3 above) and so-called 'fuzzy logic tools' yielded somewhat disappointing results. For example, the authors of Ref. [181] predicted that the next GLE after GLE71 should occur in the first half of 2015, but real GLE 72 took place only on 10 September 2017.

Practically important aspects of space weather related to the enhanced GLE occurrence rate in SA cycle 23 were considered in detail in Ref. [182]. This article reported results of calculations of the radiation dose for aircraft flying transpolar routes from individual GLEs of the preceding cycle. Of special interest are effects of cosmic weather during the large solar events in October and November 2003. The authors emphasize the importance of using NM data for forecasting SPEs in the region of the most radiation-hazardous SCR energies (tens and hundreds of MeV). This prognosis permits aircraft and spacecraft crews to be alerted in advance about the risk of irradiation exposure. It is worthwhile to mention in this context calculations of radiation doses from the 15.04.2001 and 20.01.2005 GLEs for three real airline routes by the methods of five different research groups based in Apatity, Athens, Bern, Kiel, and Hobart [183]. The results proved dismally inconsistent, which suggests serious methodical problems hampering the analysis and application of NM data. The discrepancies are mostly due to incorrect determination and interpretation of the shape of SCR spectra in Earth's orbit in different phases of the proton event.

In the past few years, researchers interested in the development of prognostic schemes have paid increasingly more attention to proton fluxes (fluences) with energies $\geqslant 100$ MeV [178] and $\geqslant 200$ MeV [184]. Also used are the $\Phi(\geqslant 30\ \text{MeV})/\Phi(\geqslant 200\ \text{MeV})$ ratios (see, for instance, Ref. [184]). Notice that such an analysis is carried out 'inside' the SCR spectrum for a given event that *has already formed* near Earth. Therefore, its results are of low prognostic value. At the same time, they can be useful for understanding the nature of SCR spectral breaks [157].

9. Summing up...

Summarizing the above, some conclusions can be made and future tasks and remaining problems of SCR research outlined.

9.1 Future tasks and/or unresolved problems

A pressing question of modern GLE physics was formulated in a special issue of *Space Science Reviews* [vol. 171, 2012] as follows: "What should be peculiar conditions on the Sun to enable GLE generation?" The author of paper [113] tends to think that the PC in the GLE originates from flares in the lower corona, whereas the delayed component can be generated it two ways: one being prolonged acceleration and/or capture of particles in the flare region, the other acceleration at the coronal and interplanetary shock waves. On the other hand, it is argued in Ref. [114] that there is no reliable evidence yet of a correlation between GLE amplitude and parameters of flares or CMEs.

At the same time, there are solid arguments in favor of the hypothesis of shock wave formation in the corona prior to GLE, just before particle liberation. Particles are released when CMEs reach a mean height of $\sim 3.09 R_S$, at least for magneto-conjugate solar sources (W20–W90). The authors of Ref. [185] used the model of a potential field at the source surface (PFSS) and concluded that only half of all GLEs are well magneto-conjugate to the sources. At the same time, neither CME and flare power nor the degree of complexity of the Sun's active regions create the sufficient conditions for the onset of GLE. It was shown in Ref. [186] that the large event of 20 January 2005 (GLE69) could have had two sources, a flare and the accompanying CME.

An interesting feature of GLE reported in Ref. [187] was that only around 50% of the events exhibited common properties with ^{3}He-rich impulsive SPEs, including enrichment with other ions (enhanced Ne/O, Fe/O, ^{22}Ne/^{20}Ne ratios) and the high charge state of Fe ions. It is supposed that such events contribute to the seed population of particles that are later accelerated at the CME-generated shock waves. The authors of Ref. [188] proposed a GLE generation scenario in which two GLEs interact on the condition that they were sequentially expelled from the corona over one and the same active region. The first CME was assumed to be narrower and slower than the second. As soon as the second CME overtakes the first one, their magnetic structures become reconnected, which enhances acceleration effect at two shock waves from the combination of two CMEs.

The only conclusion presumably acceptable to all GLE researchers was formulated a few years ago [26] and reduces to the rapidly developing GLE concept ('evolving paradigm').

The detailed physical picture of the processes leading to the double-peaked structure of GLE awaits clarification. We are of the opinion that the hypothesis of the interplanetary origin of two components is insufficient to fundamentally solve the problem. Also, there are compelling reasons to accept the model of two solar sources as the main SCR generation model. Evidently, this proposal complies with, rather than contradicts, the modern concept of a particle multiple acceleration on the Sun.

9.2 Prospects for SCR research

The prospects for further studies in this field of solar–terrestrial physics are readily apparent from the fact that many fundamental problems of particle acceleration physics (at the micro- and macro-levels) remain unresolved despite the 75-year history of SCR research. The list of such problems includes the duration and strength of injection of accelerated particles and the relative roles of particle acceleration and capture (retention), i.e., event duration. Further studies on the variation of the elemental composi-

tion and charge state of accelerated particles from one event to another are needed.

The scope of SCR research and applications of the data obtained is far wider than outlined in the preceding paragraphs. Suffice it to mention that problems pertinent to the generation of neutrons and gamma radiation of solar flares (see, for instance, Refs [15, 189–193]) are directly related to the physics of acceleration and localization of SCR sources on the Sun, etc. However, they go far beyond the scope of the present review. By way of example, the source of the 2.223-MeV line radiation in GLE42 remains to be identified [35, 194]. As mentioned above, investigations into minor SCR events based on ground-based observations are of special importance, as exemplified by the small GLE54 of 2 November 1992 with a high geomagnetic threshold (cut-off rigidity of ~ 7.5 GV) recorded by the Mexico station [195].

The most serious challenge facing researchers is those GLEs that were accompanied by prolonged (2 hours) high-energy (up to 2 GeV) gamma radiation. Such events are exemplified by GLE51 and GLE52 recorded on 11 and 15 June 1991, respectively [196, 197]. In light of the preceding discussion, a long-standing acceleration of SCRs and/or their protracted retention (emission) appear highly unlikely. Nevertheless, the possibility of post-eruptive acceleration, at least in two steps, cannot be ruled out (see, for instance, Refs [198, 199]).This approach leads to a new GLE concept (see Section 4) and is consistent with another, more general, paradigm of multiple particle acceleration under solar conditions [93]. Notice, however, that the available data on neutrons and gamma radiation give evidence of particle acceleration up to relativistic energies in flares rather than at shock fronts accompanying CMEs

The authors of some recent statistical studies (see, e.g., Refs [200, 201]) arrived at a similar conclusion. Reference [200] demonstrated, based on the analysis of 44 SPEs in a 15–40-MeV energy range, that flares play a key role in proton acceleration up to high energies. This inference is confirmed by the results of a statistical analysis [201] of the relationship between fluences of 35-GHz microwave bursts and $E > 100$-MeV proton fluences. Shock acceleration appears to prevail in weak events, even if it is of less consequence at high energies where the events observed are related to powerful solar flares. This means that the traditional contraposition of particle acceleration in flares and at shock waves should give way to a new well-reasoned approach (see Fig. 3).

A plausible assertion about the known flare–CME dilemma (Sections 2.3 and 4.1) is difficult to make, since it remains unresolved. Clearly, both represent two sides of the same phenomenon, namely a strong 'explosion' in the solar atmosphere, understood not in the conventional sense of the word but as a specific electrodynamic process in a high-temperature plasma 'permeated' by a strong magnetic field [85, 87]. Current multiwave observations of the Sun give evidence that this process is characterized by a number of specific features (see, for instance, Refs [87, 202]). As far as SCR generation is concerned, of special interest is energy distribution among participants in this process, e.g., part of the energy carried away by accelerated particles in various acceleration models.

Important geophysical applications include detailed investigations into the still poorly explored SCR effects in Earth's atmosphere considered in Refs [138, 170], taking advantage of modern monitoring techniques with the use of space probes. Criticism of 'space climatology' [203] is to be noted, taking into consideration that it questions the possibility of a relationship between cosmic ray ionization of the atmosphere and aerosol (cloud) formation.

Enormous quantities of observational data have been collected during decades of SCR research that yielded fundamental information about physical processes in the Sun and outer space. For example, the possibility of proton acceleration in stellar atmospheres was demonstrated long before the discovery of synchrotron radiation from remote galactic sources.

In other words, SCR research over the last decades has revealed close and miscellaneous connections ('interpenetration') between SCRs and phenomena of stellar physics at large, cosmic plasma physics, geophysics, general physics (including particle acceleration), etc.

SCRs remain the center of interest and activity in the face of challenges associated with the global problems of the Sun's evolution as a star, its past activity, the possible contribution of extreme solar flares to the evolution of the biosphere, etc. In short, SCR studies always were and remain one of the most efficient tools for solar physics research and elucidation of solar–terrestrial relationships.

In conclusion, we all must feel profound appreciation toward a few generations of researchers who for many years managed and continue to maintain the work of the worldwide network of CR stations. The author is pleased to express gratitude to the entire international community of SCR scientists and all his colleagues engaged in space physics from many countries, whose ideas, results, and materials were used in the present article. Special thanks are due to my co-workers in the Soviet (Russian) 'Catalogue' Working Group that has prepared and published (since the early 1980s) several SPE catalogs covering the period from 1970 to 2009 (more than four cycles of solar activity). The author is grateful to the independent reviewer for constructive criticism and valuable comments.

Addendum

Extreme solar events: myth or reality? It is how the fundamental problem has to be defined that has aroused considerable interest among researchers, including astrophysical theorists [204–207], glaciologists and climate scientists [159, 160], and specialists in radiation protection of space missions [208]. The matter is of great consequence indeed. Tens of articles have been published on the topic over the last five years. Of special importance are those providing a critical insight into the methodical aspects of investigations of ancient SPEs. The nitrate method is subjected to the most severe criticism.

The AD775 event [162–164], SPE 994AD [209, 210], and 3372 BC [211] documented based on radiocarbon analysis occurred after the publication of the first indirect (proxy) data on proton fluences $\Phi(\geqslant 30\ \text{MeV})$ [155], including the Carrington event AD1859 obtained by the nitrate method. Despite the limitations of these data, the authors of Ref. [157] thought fit to use them to construct the new SPE distribution function making use of $\Phi(\geqslant 30\ \text{MeV})$ fluences (Fig. 19) and taking into consideration recent estimates for the AD775 event [212] and limiting fluence from SCRs [213] for the biggest SPEs.

Reference [155] was preceded by attempts to associate nitrate ion spikes detected in Greenland and Antarctic ice core samples with large SPEs [153, 154, 158].It was found that

the peaks are only a few weeks behind major SPEs, in particular after the first four GLEs [154]. A few years later, these publications provoked an ardent discussion on the possibility of using the nitrate method for the identification of ancient SPEs and estimation of fluences. The authors of Ref. [159] questioned the possibility of any 'nitrate signal' from the AD1859 event and attributed it to ash deposition during wildfires in North America. This inference was challenged in Ref. [214] based on the fact that the authors of Ref. [159] relied upon low-temporal resolution data. Soon, new arguments against assertions in Ref. [214] were advanced [215], to the effect that data on ^{10}Be content provide more adequate information even if with a lower resolution.

Finally, a detailed survey [216] is worthy of note in which the so-called Whole Atmosphere Community Climate Model (WACCM) was used to comprehensively address the question "How strong should an SPE be to generate as many nitrates in the atmosphere as necessary to be detected by modern methods?" The conclusion made in Ref. [216] sounds like a death sentence to the nitrate method on the grounds that nitrates cannot serve as indirect (proxy) indicators of ancient SPEs, and the results obtained in these studies must be rejected as invalid. The authors of Ref. [217], based on modeling and measurements in different polar ice core samples, failed to detect a nitrate signal from AD 775, believed to be thus far the greatest of known ancient SPEs, despite the high temporal resolution of measurements (up to 20 samples/year) and exclusion of the processes that occurred after nitrate deposition. The authors of Ref. [218], in turn, concluded after analysis of nitrate data for AD775 and events of the years 994, 1859, and 1956 that none of them produced a readable (measurable) signal.

This, however, does not rule out the possibility of using nitrate data, e.g., for the study of long-term GCR variations [219]. Moreover, wavelet analysis has revealed a high degree of coherence between ^{10}Be peaks and nitrate content. The preferential relationship between ^{10}Be and nitrates (compared with other chemical constituents of the atmosphere) can be attributed to their common cosmogenic origin. It is pertinent to emphasize here a variety of nitrate generation sources in the terrestrial atmosphere (see, for instance, Ref. [220]), the multidisciplinary character of the problem in question [221], and a large number of unexplored aspects of SCR–atmosphere interaction [138, 216, 222].

In conclusion, there are a few interesting quotes from Ref. [223]. One states an obvious fact that opinions differ: some researchers are ready to rely on proxy data, whereas others regard them as 'mere noise'. The generation of cosmogenic components of the atmosphere depends on solar activity and (at large time-scales) the strength of the geomagnetic field. However, the resulting cosmogenic signal is not immediately and directly recorded in natural archives; on the contrary, newly formed cosmogenic radionuclides are from the very beginning involved in a variety of transport processes that modify the primary signal. For those interested in SPEs, these modifications are nothing more than noise, because they tend to distort the SCR signal of interest. Conversely, they are of great value for a physicist or chemist studying atmospheric processes, because they may help improve atmospheric circulation (mixing) models and thereby promote the understanding of the interaction between the stratosphere and troposphere.

In the end, the author deems it untimely to altogether abandon the nitrate method for the detection of ancient SPEs. Suffice it to recall that all currently available data are indirect by definition, and fluence estimates strongly depend on the scenario of the event being considered. The purpose is to adequately take into account such SPE features of a major event (like that of 20 January 2005) as SCR intrusion N/S anisotropy, energy spectrum, and duration [224]. Hopefully, it will be possible to quantify the relative contribution of SPEs to the total nitrate signal.

References

1. Lange I, Forbush S E *J. Geophys. Res.* **47** 331 (1942)
2. Simpson J A, in *Proc. of the 21st Intern. Cosmic Ray Conf., Adelaide, Australia, January 6–19, 1990* Vol. 12 (Adelaide: Adelaide Univ., 1990) p. 187
3. Elliot H, in *Progress in Cosmic Ray Physics* Vol. 1 (Eds J G Wilson, S A Wouthuysen) (Amsterdam: North-Holland Publ. Co., 1952) p. 455
4. Dorman L I *Variatsii Kosmicheskikh Luchei* (Cosmic Rays: Variations) (Moscow: GITTL, 1957)
5. Dorman L I *Cosmic Rays: Variations and Space Explorations* (Amsterdam: North-Holland, 1974); Translated from Russian: *Variatsii Kosmicheskikh Luchei i Issledovanie Kosmosa* (Moscow: Izd. AN SSSR, 1963)
6. Dorman L I *Nuovo Cimento* **8** (Suppl. 2) 391 (1958)
7. Carmichael H *Space Sci. Rev.* **1** 28 (1962)
8. Dorman L I, Miroshnichenko L I *Solnechnye Kosmicheskie Luchi* (Solar Cosmic Rays) (Moscow: Nauka, 1968)
9. Sakurai K *Physics of Solar Cosmic Rays* (Tokyo: Univ. of Tokyo Press, 1974)
10. Pomerantz M A, Duggal S P *Rev. Geophys.* **12** 343 (1974)
11. Duggal S P *Rev. Geophys.* **17** 1021 (1979)
12. Dorman L I, Venkatesan D *Space Sci. Rev.* **64** 183 (1993)
13. Reames D V *Space Sci. Rev.* **90** 413 (1999)
14. Ryan J M, Lockwood J A, Debrunner H *Space Sci. Rev.* **93** 35 (2000)
15. Miroshnichenko L I, Perez-Peraza J A *Int. J. Mod. Phys. A* **23** 1 (2008)
16. Miroshnichenko L I, Vashenyuk E V, Pérez-Peraza J A *Geomagn. Aeron.* **53** 541 (2013); *Geomagn. Aeron.* **53** 579 (2013)
17. Miroshnichenko L I *Solar Cosmic Rays* (Dordrecht: Kluwer Acad. Publ., 2001)
18. Miroshnichenko L I *Radiation Hazard in Space* (Dordrecht: Kluwer Acad. Publ., 2003)
19. Miroshnichenko L I *Fizika Solntsa i Solnechno-Zemnykh Svyazei* (Physics of the Sun and Solar-Terrestrial Relationships) (Moscow: Univ. Kniga, 2011)
20. Miroshnichenko L *Solar Cosmic Rays: Fundamentals and Applications* 2nd ed. (New York: Springer, 2014)
21. Miroshnichenko L I, in *Elektromagnitnye i Plazmennye Protsessy ot Nedr Solntsa do Nedr Zemli* (Ed. V D Kuznetsov) (Moscow: IZMIRAN, 2015) p. 285
22. Forbush S E *Phys. Rev.* **70** 771 (1946)
23. Adams N *Philos. Mag. 7* **41** 503 (1950)
24. Forbush S E, Stinchcomb T B, Schein M *Phys. Rev.* **79** 501 (1950)
25. Krasil'nikov D D, Kuz'min A I, Shafer Yu G "Variatsii intensivnosti kosmicheskikh luchei" ("Variations of cosmic ray intensity") *Tr. Yakutskogo Filiala Akad. Nauk SSSR, Ser. Fiz.* (1) 41 (1955)
26. Cliver E W *Proc. IAU* **4** (S257) 401 (2008)
27. Chupp E L *AIP Conf. Proc.* **374** 3 (1996)
28. Hey J S *Nature* **157** 47 (1946)
29. Smart D F, Shea M A *J. Spacecraft Rockets* **26** 403 (1989)
30. Krivonosov Yu I *Phys. Usp.* **43** 949 (2000); *Usp. Fiz. Nauk* **170** 1021 (2000)
31. Gubarev V *Belyi Arkhipelag Stalina. Dokumental'noe Povestvovanie o Sozdanii Yadernoi Bomby, Osnovannoe na Rassekrechennykh Materialakh "Atomnogo Proekta SSSR"* (Stalin's White Archipelago. The Documented Story About Creation of Nuclear Bomb Based on Declassified Materials of the USSR Atomic Project) (Moscow: Molodaya Gvardiya, 2004)
32. Hess V F *Phys. Z.* **13** 1084 (1912)
33. Dorman IV *Kosmicheskie Luchi* (Cosmic Rays) (Moscow: Nauka, 1981)

34. Dorman I V, Dorman L I *Adv. Space Res.* **53** 1388 (2014)
35. Carmichael H "Cosmic Rays (Instruments)", in *Annals of the International Years of the Quiet Sun, IQSY* Vol. 1 (Ed. C M Minnis) (Cambridge, MA: MIT Press, 1968) p. 178
36. Krymskii G F et al. *Dokl. Akad. Nauk SSSR* **314** 824 (1990)
37. Swinson D B, Shea M A *Geophys. Res. Lett.* **17** 1073 (1990)
38. Miroshnichenko L I, De Koning C A, Perez-Enriquez R *Space Sci. Rev.* **91** 615 (2000)
39. Karpov S N, Miroshnichenko L I, Vashenyuk E V *Nuovo Cimento C* **21** 551 (1998)
40. Flückiger E O et al., in *Proc. 16th European Cosmic Ray Symp.* (Ed. J Medina) (Alcalá de Henares: Alcala Univ. Press, 1998) p. 219
41. Miroshnichenko L I *Geomagn. Aeron.* **34** 29 (1994)
42. Schindler S M, Kearney P D, in *Proc. of the 13th Intern. Conf. on Cosmic Rays, Denver, CO, USA, 17–30 August 1973* Vol. 2 (Denver, CO: Univ. of Denver, Dept. of Physics and Astronomy, 1973) p. 1554
43. Smart D F, Shea M A *Adv. Space Res.* **17** 113 (1996)
44. Vashenyuk E V et al. *Geomagn. Aeron.* **48** 149 (2008); *Geomagn. Aeron.* **48** 157 (2008)
45. Balabin Yu V et al. *Bull. Russ. Acad. Sci. Phys.* **73** 304 (2009); *Izv. Ross. Akad. Nauk, Ser. Fiz.* **73** 321 (2009)
46. Timashkov D A et al., in *Proc. of the 30th Intern. Cosmic Ray Conf., July 3–11, 2007, Mérida, Yucatán, Mexico* Vol. 1 (Eds R Caballero et al.) (Mexico City, Mexico: Univ. Nacional Autónoma de México, 2008) p. 209
47. Abbasi R et al. (IceTop Collab.) *Astrophys. J. Lett.* **689** L65 (2008)
48. Gosling J T *J. Geophys. Res.* **98** 18937 (1993)
49. Belov A V et al., in *Elektromagnitnye i Plazmennye Protsessy ot Nedr Solntsa do Nedr Zemli* (Electromagnetic and Plasma Processes from the Sun to the Core of the Earth) (Exec. Ed. V V Migulin) (Moscow: Nauka, 1989) p. 49
50. Li C et al. *Astrophys. J.* **770** 34 (2013)
51. Reames D V *Rev. Geophys.* **33** (S1) 585 (1995)
52. Shea M A, Smart D F, in *Biological Effects and Physics of Solar and Galactic Cosmic Radiation* (NATO ASI Series, Ser. B, Vol. 243, Eds C E Swenberg, G Horneck, E G Stassinopoulos) (New York: Plenum Press, 1993) p. 37
53. Smart D F, Shea M A *Solar Phys.* **16** 484 (1971)
54. Dodson H W et al. *Catalogue of Solar Particle Events 1955 – 1969* (Astrophysics and Space Science Library, Vol. 49, Eds Z Švestka, P Simon) (Dordrecht: Kluwer Acad., 1975)
55. Akinyan S T et al. *Catalogue of Solar Proton Events 1970 – 1979* (Ed. Yu I Logachev) (Moscow: Nauka, IZMIRAN, 1983)
56. Bazilevskaya G A et al. *Catalogue of Energetic Spectra of Solar Proton Events 1970 – 1979* (Ed. Yu I Logachev) (Moscow: Nauka, 1986)
57. Bazilevskaya G A et al. *Catalogue of Solar Proton Events 1980 – 1986* Pts 1, 2 (Ed. Yu I Logachev) (Moscow: World Data Center B-2, 1990)
58. Sladkova A I *Radiat. Measur.* **26** 447 (1996)
59. Sladkova A I et al. *Catalogue of Solar Proton Events 1987 – 1996* (Ed. Yu I Logachev) (Moscow: Univ. Press, 1998)
60. Logachev Yu I et al. *Catalogue of Solar Proton Events in the 23rd Cycle of Solar Activity. 1996 – 2008* (Ed. Yu I Logachev) (Moscow: World Data Centers, 2016); http://www.wdcb.ru/stp/data/SPE/Catalog_SPE_23_cycle_SA.pdf
61. NOAA Space Environment Center. Solar Proton Events Affecting the Earth Environment: Preliminary Listing 1976–present (2018), http://umbra.nascom.nasa.gov/SEP/
62. Miroshnichenko L I, Karpov S N *Geomagn. Aeron.* **44** 554 (2004); *Geomagn. Aeron.* **44** 601 (2004)
63. Li C, Miroshnichenko L I, Fang C *Res. Astron. Astrophys.* **15** 1036 (2015)
64. Atwell W et al., in *45th Intern. Conf. on Environmental Systems, ICES 2015, July 12–16, 2015, Bellevue, WA, USA*, p. 340
65. Cliver E W, Dröge W, Müller-Mellin R *J. Geophys. Res.* **98** 15231 (1993)
66. Kahler S W et al *J. Geophys. Res.* **89** 9683 (1984)
67. Kallenrode M-B, Cliver E W, in *Proc. of the 27th Intern. Cosmic Ray Conf., 7–15 August, 2001, Hamburg, Germany* Vol. 8 (Berlin: Copernicus Gesellschaft, 2001) p. 3314; in *Proc. of the 27th Intern. Cosmic Ray Conf., 7–15 August, 2001, Hamburg, Germany* Vol. 8 (Berlin: Copernicus Gesellschaft, 2001) p. 3318
68. Filippov A T, Chirkov N P *Izv. Akad. Nauk SSSR, Ser. Fiz.* **42** 1078 (1978)
69. Kuz'min A I, Filippov A T, Chirkov N P *Izv. Akad. Nauk SSSR, Ser. Fiz.* **47** 1703 (1983)
70. Ellison D C, Ramaty R *Astrophys. J.* **298** 400 (1985)
71. Simnett G M *Phil. Trans. R. Soc. London A* **336** 439 (1991)
72. Mewaldt R A et al. *J. Geophys. Res.* **110** A09S18 (2005)
73. Mewaldt R A *Space Sci. Rev.* **124** 303 (2006)
74. Mewaldt R A et al., in *Proc. of the 30th Intern. Cosmic Ray Conf., July 3–11, 2007, Mérida, Yucatán, Mexico* Vol. 1 (Eds R Caballero et al.) (Mexico City, Mexico: Univ. Nacional Autónoma de México, 2008) p. 1167
75. Band È et al. *Astrophys. J.* **413** 281 (1993)
76. Karpov S N, Miroshnichenko L I, in *Proc. of the 30th Intern. Cosmic Ray Conf., July 3–11, 2007, Mérida, Yucatán, Mexico* Vol. 1 (Eds R Caballero et al.) (Mexico City, Mexico: Univ. Nacional Autónoma de México, 2008) p. 413
77. Miroshnichenko L I *Radiat. Measur.* **26** 421 (1996)
78. Struminskii A B, in *Solnechnaya i Solnechno-Zemnaya Fizika — 2015. XIX Vseross. Ezhegodnaya Konf. po Fizike Solntsa, 5–9 Oktyabrya 2015, Sankt-Peterburg, Rossiya. Trudy* (Solar and Solar-Terrestrial Physics — 2015. XIX All-Russian Annual Conf. on the Physics of the Sun, October 5–9, 2015, St. Petersburg, Russia. Proc.) (Exec. Eds A V Stepanov, Yu A Nagovitsin) (St. Petersburg: The Central Astronomical Observatory of the Russian Academy of Sciences at Pulkovo, 2015) p. 343
79. Syrovatskii S I *Sov. Phys. JETP* **13** 1257 (1961); *Zh. Eksp. Teor. Fiz.* **40** 1788 (1961)
80. Wang R *Astropart. Phys.* **31** 149 (2009)
81. Perez-Peraza J A *Geomagn. Aeron.* **32** (2) 1 (1992)
82. Syrovatskii S I *Sov. Astron.* **10** 270 (1966); *Astron. Zh.* **43** 340 (1966)
83. Syrovatskii S I *Sov. Phys. JETP* **23** 754 (1966); *Zh. Eksp. Teor. Fiz.* **50** 1133 (1966)
84. Syrovatskii S I *Solar Phys.* **76** 3 (1982)
85. Somov B V *Phys. Usp.* **53** 954 (2010); *Usp. Fiz. Nauk* **180** 997 (2010)
86. Frank A G *Phys. Usp.* **53** 941 (2010); *Usp. Fiz. Nauk* **180** 982 (2010)
87. Somov B V *Plasma Astrophysics* Pt. I *Fundamentals and Practice* Astrophysics and Space Science Library, Vol. 391) 2nd ed. (New York: Springer, 2013); *Plasma Astrophysics* Pt. II *Reconnection and Flares* (Astrophysics and Space Science Library, Vol. 392) 2nd ed. (New York: Springer, 2013)
88. Priest E, Forbes T *Magnetic Reconnection: MHD Theory and Applications* (Cambridge: Cambridge Univ. Press, 2000); Translated into Russian: *Magnitnoe Peresoedinenie* (Moscow: Fizmatlit, 2005)
89. Somov B V, Oreshina A V *Bull. Russ. Acad. Sci., Ser. Phys.* **75** 735 (2011); *Izv. Ross. Akad. Nauk, Fiz.* **75** 784 (2011)
90. Gopalswamy N, Nitta N V *Space Sci. Rev.* **171** 1 (2012)
91. Pérez-Peraza J et al. *Astrophys. J.* **695** 865 (2009)
92. Kahler S *Astrophys. J.* **428** 837 (1994)
93. Miroshnichenko L I *Izv. Ross. Akad. Nauk, Ser. Fiz.* **67** 400 (2003)
94. Toptygin I N *Cosmic Rays in Interplanetary Magnetic Fields* (Dordrecht: D. Reidel, 1985); Translated from Russian: *Kosmicheskie Luchi v Mezhplanetnykh Magnitnykh Polyakh* (Moscow: Nauka, 1983)
95. Vashenyuk E V, Balabin Yu V, Gvozdevsky B B *Astrophys. Space Sci. Trans.* **7** 459 (2011)
96. Miroshnichenko L I *J. Moscow Phys. Soc.* **7** 17 (1997)
97. Vashenyuk E V et al., in *Proc. of the 25th Intern. Cosmic Ray Conf., 30 July – 6 August, 1997, Durban, South Africa* Vol. 1 (Eds M S Potgieter, C Raubenheimer, D J van der Walt) (Transvaal, South Africa: Potchefstroom Univ., 1997) p. 161
98. Podgorny I M et al. *J. Atmos. Solar-Terr. Phys.* **72** 988 (2010)
99. Krymskii G F *Sov. Phys. Dokl.* **22** 327 (1977); *Dokl. Akad. Nauk SSSR* **234** 1306 (1977)
100. Zank G P, Rice W K M, Wu C C *J. Geophys. Res.* **105** 25079 (2000)
101. Berezhko E G, Taneev S N *Astron. Lett.* **29** 530 (2003); *Pis'ma Astron. Zh.* **29** 601 (2003)
102. Berezhko E G, Taneev S N *Astron. Lett.* **39** 393 (2013); *Pis'ma Astron. Zh.* **39** 443 (2013)

103. Krymsky G F et al. *JETP Lett*. **102** 335 (2015); *Pis'ma Zh. Eksp. Teor. Fiz*. **102** 372 (2015)
104. Berezhko E G, Krymskii G F *Sov. Phys. Usp*. **31** 27 (1988); *Usp. Fiz. Nauk* **154** 49 (1988)
105. Berezhko E G et al. *Astron. Lett*. **22** 260 (1996); *Pis'ma Astron. Zh*. **22** 290 (1996)
106. Shea M A, Smart D F *AIP Conf. Proc*. **374** 131 (1996)
107. Shea M A, Smart D F, in *Proc. of the 25th Intern. Cosmic Ray Conf., 30 July – 6 August, 1997, Durban, South Africa* Vol. 1 (Eds M S Potgieter, C Raubenheimer, D J van der Walt) (Transvaal, South Africa: Potchefstroom Univ., 1997) p. 129
108. Nemzek R J et al. *J. Geophys. Res*. **99** 4221 (1994)
109. Fedorov Yu I et al., in *Proc. of the 25th Intern. Cosmic Ray Conf., 30 July – 6 August, 1997, Durban, South Africa* Vol. 1 (Eds M S Potgieter, C Raubenheimer, D J van der Walt) (Transvaal, South Africa: Potchefstroom Univ., 1997) p. 193
110. Cliver E W et al. *Astrophys. J*. **260** 362 (1982)
111. Kahler S W, Simnett G M, Reiner M J, in *Proc. of the 28th Intern. Cosmic Ray Conf., July 31 – August 7, 2003, Tsukuba, Japan* Vol. 7 (Eds T Kajita et al.) (Tokyo: Universal Acad. Press, 2003) p. 3415
112. Bazilevskaya G A *Adv. Space Res*. **43** 530 (2009)
113. Aschwanden M J *Space Sci. Rev*. **171** 3 (2012)
114. Gopalswamy N et al. *Space Sci. Rev*. **171** 23 (2012)
115. Kuznetsov S N et al. *Solar Phys*. **268** 175 (2011)
116. Struminsky A B, Zimovets I V *Bull. Russ. Acad. Sci., Ser. Phys*. **73** 315 (2009); *Izv. Ross. Akad. Nauk, Ser. Fiz*. **73** 332 (2009)
117. Klecker B *J. Phys. Conf. Ser*. **409** 012015 (2013)
118. Cane H V et al. *J. Geophys. Res*. **111** A06S90 (2006)
119. Meyer J-P *Astrophys. J. Suppl*. **57** 151 (1985)
120. Laming J M *Astrophys. J*. **614** 1063 (2004)
121. Tomozov V M, in *Solnechno-Zemnaya Fizika* (Solar-Terrestrial Physics) Iss. 20 (Novosibirsk: Izd. SO RAN, 2012) p. 19
122. Desai M I et al. *Space Sci. Rev*. **130** 243 (2007)
123. Cohen C M S et al. *J. Geophys. Res*. **110** A09S16 (2005)
124. Desai M, Giacalone J *Living Rev. Solar Phys*. **13** 3 (2016)
125. Cane H V et al. *J. Geophys. Res*. **111** A06S90 (2006)
126. Tylka A J et al. *Astrophys. J*. **625** 474 (2005)
127. Kahler S W et al. *Space Sci. Rev*. **171** 121 (2012)
128. Kahler S W *J. Geophys. Res*. **87** 3439 (1982)
129. Battaglia Û, Grigis P C, Benz A O *Astron. Astrophys*. **439** 737 (2005)
130. Mitra-Kraev U et al. *Astron. Astrophys*. **431** 679 (2005)
131. Chiba N et al. *Astropart. Phys*. **1** 27 (1992)
132. Struminsky A, Matsuoka M, Takahashi K *Astrophys. J*. **429** 400 (1994)
133. Miyasaka H et al., in *Proc. of the 29th Intern. Cosmic Ray Conf., August 3–10, 2005, Pune, India* Vol. 1 (Eds B S Acharya et al.) (Mumbai: Tata Institute of Fundamental Research, 2005) p. 241
134. Sako et al. *Astrophys. J. Lett*. **651** L69 (2006)
135. Miroshnichenko L I, Yanke V G *Solar Phys*. **291** 3685 (2016)
136. Gnevyshev M N *Solar Phys*. **51** 175 (1977)
137. Miroshnichenko L I *Adv. Space Res*. **36** 1742 (2005)
138. Mironova I A et al. *Space Sci. Rev*. **194** 1 (2015)
139. Miroshnichenko L I et al. *Geomagn. Aeron*. **52** 547 (2012); *Geomagn. Aeron*. **52** 579 (2012)
140. Gupta M, Mishra V K, Mishra A P *J. Geophys. Res*. **112** A05105 (2007)
141. Nagashima K, Sakakibara S, Morishita I *J. Geomagn. Geoelectr*. **43** 685 (1991)
142. Miroshnichenko L I *Izv. Ross. Akad. Nauk, Ser. Fiz*. **67** 462 (2003)
143. Maehara H et al. *Nature* **485** 478 (2012)
144. Shibata K et al. *Publ. Astron. Soc. Jpn*. **65** 49 (2013)
145. Aschwanden M J, Freeland S L *Astrophys. J*. **754** 112 (2012)
146. Aschwanden M J *Astron. Astrophys*. **539** A2 (2012)
147. Aschwanden M J et al. *Astrophys. J*. **535** 1047 (2000)
148. Shimizu T *Publ. Astron. Soc. Jpn*. **47** 251 (1995)
149. Crosby N B, Aschwanden M J, Dennis B R *Solar Phys*. **143** 275 (1993)
150. Shea M A, Smart D F *Solar Phys*. **127** 297 (1990)
151. Damon P E, Long A, Wallick E I *Earth Planet. Sci. Lett*. **20** 300 (1973)
152. Fan C Y et al., in *Proc. of the 19th Intern. Cosmic Ray Conf., 11–23 August 1985, San Diego, CA* Vol. 5 (Washington, DC: NASA, 1985) p. 371
153. Dreschhoff G A M, Zeller E J *Solar Phys*. **127** 333 (1990)
154. Kepko L et al. *J. Atmos. Solar-Terr. Phys*. **71** 1840 (2009)
155. McCracken K G et al. *J. Geophys. Res*. **106** 21585 (2001)
156. Townsend L W et al. *Adv. Space Res*. **38** 226 (2006)
157. Miroshnichenko L I, Nymmik R A *Radiat. Measur*. **61** 6 (2014)
158. Smart D F, Shea M A, McCracken K G *Adv. Space Res*. **38** 215 (2006)
159. Wolff E W et al. *Geophys. Res. Lett*. **39** L08503 (2012)
160. Schrijver C J et al. *J. Geophys. Res*. **117** A08103 (2012)
161. Usoskin I G, Kovaltsov G A *Astrophys. J*. **757** 92 (2012)
162. Miyake F et al. *Nature* **486** 240 (2012)
163. Usoskin I G et al. *Astron. Astrophys*. **552** L3 (2013)
164. Jull A J T et al. *Geophys. Res. Lett*. **41** 3004 (2014)
165. Thomas B C et al. *Geophys. Res. Lett*. **40** 1237 (2013)
166. Pavlov A K et al. *Mon. Not. R. Astron. Soc*. **435** 2878 (2013)
167. Cliver E W et al. *Astrophys. J*. **781** 32 (2014)
168. Pavlov A K et al. *Astrophys. Lett*. **40** 640 (2014); *Pis'ma Astron. Zh*. **40** 706 (2014)
169. Király P, Wolfendale A W, in *Proc. of the 26th Intern. Cosmic Ray Conf., ICRC, August 17–25, 1999, Salt Lake City, Utah, USA* Vol. 6 (Eds D Kieda, M Salamon, B Dingus) (New York: AIP, 1999) p. 163
170. Miroshnichenko L I *J. Atmos. Solar-Terr. Phys*. **70** 450 (2008)
171. Quack M et al., in *Proc. of the 27th Intern. Cosmic Ray Conf., 7–15 August, 2001, Hamburg, Germany* Vol. 10 (Berlin: Copernicus Gesellschaft, 2001) p. 4023
172. Kirillov A S et al., in *Proc. of the 30th Intern. Cosmic Ray Conf., July 3–11, 2007, Mérida, Yucatán, Mexico* Vol. 1 (Eds R Caballero et al.) (Mexico City, Mexico: Univ. Nacional Autónoma de México, 2008) p. 773
173. Webber W R, Higbie P R, McCracken K G *J. Geophys. Res*. **112** A10106 (2007)
174. Dorman L I et al., in *Solar-Terrestrial Predictions*: *Proc. of a Workshop at Leura, Australia, October 16 – 20, 1989* (Eds R J Thompson et al.) (Boulder, CO: National Oceanic and Atmospheric Administration, Environmental Research Laboratories, 1990) p. 1386
175. Belov A V, Eroshenko E A *Radiat. Measur*. **26** 461 (1996)
176. Dorman L, Zukerman I *Adv. Space Res*. **31** 925 (2003)
177. Vashenyuk E V et al. *Bull. Russ. Acad. Sci., Ser. Phys*. **75** 770 (2011); *Izv. Ross. Akad. Nauk, Ser. Fiz*. **15** 819 (2011)
178. Veselovskii I S, Yakovchuk O S *Solar Syst. Res*. **45** 354 (2011); *Astron. Vestn*. **45** 365 (2011)
179. Mavromichalaki H et al., in *Proc. of the 31st Intern. Cosmic Ray Conf., 7–15 July 2009, Lodz, Poland* (Lodz: Univ. of Lodz, 2009) p. 4
180. Perez-Peraza J et al., in *Proc. of the 32nd Intern. Cosmic Ray Conf., ICRC2011, 11–18 August, 2011, Beijing, China* Vol. 10 (Beijing: IHEP, 2011) p. 151
181. Pérez-Peraza J, Juárez-Zuñiga A *Astrophys. J*. **803** 27 (2015)
182. Shea M A, Smart D F *Space Sci. Rev*. **171** 161 (2012)
183. Bütikofer R et al., in *Proc. of the 33rd Intern. Cosmic Ray Conf., ICRC2013, Rio de Janeiro, Brazil, July 2–9, 2013*
184. Kovaltsov G A et al. *Solar Phys*. **289** 4691 (2014)
185. Nitta N V et al. *Space Sci. Rev*. **171** 61 (2012)
186. Moraal H, McCracken K G *Space Sci. Rev*. **171** 85 (2012)
187. Mewaldt R A et al. *Space Sci. Rev*. **171** 97 (2012)
188. Li G et al. *Space Sci. Rev*. **171** 141 (2012)
189. Kuzhevskij B M, Miroshnichenko L I, Troitskaia E V *Astron. Rep*. **49** 567 (2005); *Astron. Zh*. **82** 637 (2005)
190. Tatischeff V et al. *Astrophys. J. Suppl*. **165** 606 (2006)
191. Murphy R J et al. *Astrophys. J. Suppl*. **168**167 (2007)
192. Miroshnichenko L I, Gan W Q *Adv. Space Res*. **50** 736 (2012)
193. Valdés-Galicia J F et al. *Adv. Space Res*. **43** 565 (2009)
194. Vestrand W T, Forrest D J *Astrophys. J. Lett*. **409** L69 (1993)
195. Cárdenas B V, Valdés-Galicia J F *Adv. Space Res*. **49** 1593 (2012)
196. Kanbach G et al. *Astron. Astrophys. Suppl*. **97** 349 (1993)
197. Akimov V V et al. *Solar Phys*. **166** 107 (1996)
198. Chertok I M, in *Proc. of the 24th Intern. Cosmic Ray Conf., August 28 – September 8, 1995, Rome, Italy* Vol. 4 (Eds N Iucci, E Lamanna) (Rome: IUPAP, 1995) p. 78
199. Chertok I M *J. Moscow Phys. Soc*. **7** 31 (1997)
200. Trottet G E et al. *Solar Phys*. **290** 819 (2015)
201. Grechnev V V et al. *Solar Phys*. **290** 2827 (2015)

202. Kuznetsov V D *Phys. Usp.* **53** 947 (2010); *Usp.Fiz. Nauk* **180** 988 (2010)
203. Čalogović J, Laken B A *Centr. Eur. Astrophys. Bull.* **39** 145 (2015)
204. Aulanier G et al. *Astron. Astrophys. A* **549** A66 (2013)
205. Livshits M A et al. *Adv. Space Res.* **55** 920 (2015)
206. Kitchatinov L L, Olemskoy S V *Mon. Not. R. Astron. Soc.* **459** 4353 (2016)
207. Katsova M M et al. *Astron. Rep.* **62** 72 (2018); *Astron. Zh.* **95** 78 (2018)
208. Popova E P, Kuznetsov N V, Panasyuk M I *Bull. Russ. Acad. Sci., Ser. Fiz.* **81** 173 (2017); *Izv. Ross. Akad. Nauk, Ser. Fiz.* **81** 192 (2017)
209. Miyake F, Masuda K, Nakamura T *Nature Commun.* **4** 1748 (2013)
210. Miyake F et al. *Geophys. Res. Lett.* **42** 84 (2015)
211. Wang F Y et al. *Nature Commun.* **8** 1487 (2017)
212. Mekhaldi F et al. *Nature Commun.* **6** 8611 (2015)
213. Kovaltsov G A, Usoskin I G *Solar Phys.* **289** 211 (2014)
214. Smart D F et al. *J. Geophys. Res.* **119** 9430 (2014)
215. Wolff E W et al. *J. Geophys. Res.* **121** 1920 (2016)
216. Duderstadt K A et al. *J. Geophys. Res.* **121** 2994 (2016)
217. Sukhodolov T et al. *Sci. Rep.* **7** 45257 (2017)
218. Mekhaldi F et al. *J. Geophys. Res. Atm.* **122** 11900 (2017)
219. Traversi R et al. *Sci. Rep.* **6** 20235 (2016)
220. Ogurtsov M G, Oinonen M *J. Atmos. Solar-Terr. Phys.* **109** 37 (2014)
221. Sigl M et al. *Nature* **523** 543 (2015)
222. Miroshnichenko L I *J. Atmos. Solar-Terr. Phys.* **70** 450 (2008)
223. Beer J, McCracken K, von Steiger R *Cosmogenic Radionuclides* (Berlin: Springer, 2012)
224. Krivolutsky A A, Repnev A I *Geomagn. Aeron.* **52** 685 (2012); *Geomagn. Aeron.* **52** 723 (2012)